

Capstone Report

Simple, Resilient and Low-Cost Aeroponics System for Use in
Developing Countries

Group 18: Patrick Dowd, Benjamin Strzelecki, Anas Zeid

New York University Abu Dhabi
Spring 2023

Abstract

Aerponics has emerged as a prominent sustainable alternative to traditional farming, where plants are grown in mist environments without the use of soil. In most modern applications, aerponics takes place in fully controlled environments. Although controlled environments ensure optimal conditions for efficient plant growth, the technologies used in them are too costly and advanced for many farmers in developing countries who need efficient alternatives to traditional farming to face the threats of climate change. To address this issue, we designed an aerponics system using low-cost construction materials to test the extent to which the root and leaf environments must be controlled to maintain plant conditions within an acceptable range. We monitored parameters including temperature, humidity, and CO₂ levels, using algorithms that measured real-time data from sensors. The monitoring system was also used to automatically control the pH and electrical conductivity of the nutrient solution supplied to the plants, detect faults in the system, and notify the user through a wireless communication protocol. We built and evaluated a prototype of the system based on the amount of material used, sufficient strength of the structure, thermal conductivity of material, resilience to power outages, water consumption, response of the monitoring system, technical knowledge required to operate the system, and total cost.

Acknowledgement

We would like to thank our capstone advisors Dr. Michael Davis and Dr. Khaled Shahin for continuous support in development and delivery of this project and the capstone coordinator Dr. Pradeep George for guidance on the engineering design process. Furthermore, we extend our thanks to Vijay Dhanvi, Amjad Hamad, Jorge Montalvo, Eyob Mengiste and Matthew Karau for support in design of the growing module and manufacturing the prototype. We are grateful to NYU Abu Dhabi, especially the Engineering Division and the Engineering Design Studio, for providing the facilities, resources and funding to develop and implement this project. We would like to acknowledge Kyle Wagner and Madar Farms for industry input.

Table of Contents

Abstract	i
Acknowledgment	ii
Table of Contents	iii
List of Figures	vi
List of Tables	viii
1 Problem Definition	1
1.1 Problem Analysis	1
1.2 Black-Box Modeling	2
1.2.1 Fault Prediction Subsystem	2
1.2.2 Full Aeroponics System	3
1.3 Problem Statement	4
1.4 Design Constraints	5
1.4.1 Technical Constraints	5
1.4.2 Non-Technical Constraints	6
2 Conceptualization	8
2.1 Background Research	8
2.2 Concept Generation	9
2.3 Concept Selection	10
3 Modeling, Simulation and Optimization Plan	13
3.1 Modeling Results	13
3.1.1 Structural Subsystem	14
3.1.2 Hydraulic Subsystem	16
3.1.3 Thermodynamics	18
3.1.4 Planting Subsystem	20
3.1.5 Electrical Subsystem	21
3.1.6 Software	21
3.2 Optimization Performed	22
3.2.1 Structural Subsystem	22
3.2.2 Hydraulic Subsystem	23
3.2.3 Thermodynamics	23
3.2.4 Planting Subsystem	26
3.2.5 Electrical Subsystem	26

3.2.6 Software	26
4 Final Design	27
4.1 Initial Design Proposed	27
4.1.1 Structural Subsystem	27
4.1.2 Hydraulic Subsystem	27
4.1.3 Thermodynamics	29
4.1.4 Planting Subsystem	29
4.1.5 Electrical Subsystem	29
4.1.6 Software	30
4.2 Changes Made to Initial Design	31
4.2.1 Structural Subsystem	31
4.2.2 Hydraulic Subsystem	31
4.2.3 Thermodynamics	32
4.2.4 Planting Subsystem	32
4.2.5 Electrical Subsystem	32
4.2.6 Software	33
5 Budget	35
6 Implementation	38
6.1 Report on Implementation	38
6.1.1 Structural Subsystem	38
6.1.2 Hydraulic Subsystem	39
6.1.3 Thermodynamics	39
6.1.4 Planting Subsystem	39
6.1.5 Electrical Subsystem	39
6.1.6 Software	41
6.2 Issues Faced During Implementation	45
6.2.1 Structural Subsystem	45
6.2.2 Hydraulic Subsystem	45
6.2.3 Thermodynamics	46
6.2.4 Electrical Subsystem	46
6.2.5 Software	47
6.3 Changes Made During Implementation	47
6.3.1 Structural Subsystem	47
6.3.2 Hydraulic Subsystem	47
6.3.3 Thermodynamics	48
6.3.4 Planting Subsystem	48
6.3.5 Electrical Subsystem	49
6.3.6 Software	50
6.4 Initial Results	50
6.4.1 Structural Subsystem	50
6.4.2 Hydraulic Subsystem	51
6.4.3 Thermodynamics	52
6.4.4 Planting Subsystem	52
6.4.5 Electrical Subsystem	52
6.4.6 Software	53

7 Ethics	54
8 Impact of Covid-19	55
9 Evaluation of Design	56
9.1 Criteria for Testing	56
9.2 Test Data	56
9.2.1 Size, Weight and Structural Integrity	56
9.2.2 Internal Environment Control	57
9.2.3 Water Consumption	57
9.2.4 Power Demand and Internet Connectivity	58
9.2.5 Non-Technical Constraints	59
9.3 Discussion	60
9.3.1 Size, Weight and Structural Integrity	60
9.3.2 Internal Environment Control	60
9.3.3 Water Consumption	64
9.3.4 Power Demand and Internet Connectivity	64
9.3.5 Non-Technical Constraints	65
9.3.6 Summary	66
Bibliography	68
Appendix A Project Management	69

List of Figures

1.1	Black-box model of fault detection subsystem	2
1.2	Elaborated black-box model of fault detection subsystem	3
1.3	Black-box model of full aeroponics system	3
1.4	Elaborated black-box model of full-aeroponics system	4
3.1	Flowchart for iterative design of the growing facility	13
3.2	3D model of the module in SAP 2000 with applied loads for 3 x 3 timber beams scenario	14
3.3	Shear 3D diagram for 4x4 timber structural system	15
3.4	1D heat transfer simulation through an uninsulated section of plywood cladding	19
3.5	1D heat transfer simulation through a section of the module wall insulated with polyurethane foam	20
3.6	Example of plant well design in an aeroponic system [25]	20
3.7	Example of plant well distribution in an aeroponic system [7]	21
3.8	Assignment of the final frame section properties	23
3.9	Distribution of vertical shear forces for the final timber design	24
4.1	Three-dimensional view of the growing module design	27
4.2	Cross section of the growing module design	28
4.3	Initial design of hydraulics subsystem	28
4.4	Data flow diagram of the initial software system design	30
4.5	Aluminium structure design check	31
4.6	Layout of the pump driver PCB	33
4.7	Data flow diagram of the final software system design	34
6.1	Technical drawing of the growing module	38
6.2	Germinating plants	40
6.3	Electrical circuit scheme for the growing module	40
6.4	Control system user interface	41
6.5	System parameters reading in user interface	42
6.6	Control scheme for pH and conductivity adjustment	44
6.7	Photo of the completed manufactured growing system	48
6.8	3D render of the plant bucket design	49
6.9	Vertical shear force fill diagram for the frame	51
6.10	Bending moment fill diagram for the frame	51
6.11	Observed temperature inside the module over one day	52

9.1	Observed temperatures inside and outside the module over one day. The theoretical temperature inside the module considers conduction only.	58
9.2	Observed temperature inside the module	59
9.3	Observed humidity inside the module	60
9.4	Power usage and current flow through the AC and DC subsystems of the aeroponics module over a one hour period	61
9.5	Bandwidth usage by the aeroponics module over ten minutes	62
9.6	Simulated conduction through the module's upper surface with solar radiation heat flux boundary condition	63
9.7	Work breakdown structure (WBS)	69
9.8	Dependency structure matrix (DSM)	69
9.9	Gantt chart and critical path (in orange)	71

List of Tables

2.1	Morphological chart for growing unit design	10
2.2	Pugh chart for growing technology with aeroponics as the base	11
2.3	Pugh chart for growing technology with hydroponics as the base	12
2.4	Pugh chart for growing technology with fogponics as the base	12
2.5	Pugh chart for growing technology with aquaponics as the base	12
3.1	Optimization of dimensions of short beams	22
3.2	Optimization of dimensions of long beams	23
5.1	Budget for single module with materials as per preferred design	35
5.2	Budget for Module as Implemented	37
6.1	Results for distance the solution travels from the nozzles	52
9.1	Criteria for design evaluation	57
9.2	Internal forces and moments for aluminium frame	57
9.3	Design criteria evaluation	66

Chapter 1

Problem Definition

1.1 Problem Analysis

To what extent would traditional agriculture be sufficient in providing a fresh and clean food supply for the fast-growing population under changing climatic conditions?

In the context of global warming, depletion of water resources, environmental pollution and soil degradation, the agriculture sector is faced with major challenges and is expected to undergo significant shifts in the coming years and decades [1]. If the current trends of agricultural intensification and land clearing continue, 1 billion ha of land would be cleared globally by 2050 [2]. The capacity of traditional agriculture to continuously provide a fresh and clean food supply is uncertain. Hydroponics and aeroponics are novel approaches to soil-less agriculture that provide an opportunity to meet the growing food demand in a more sustainable fashion [3].

What are some of the limitations of hydroponic and aeroponic systems?

In most modern applications, hydroponic or aeroponic cultivation takes place in controlled environments (CEA) in order to maximize yield and minimize losses of water, energy, and nutrients [4]. However, the cost of highly advanced technologies needed to implement and maintain CEA is too high for many farmers in developing countries who are most in need of novel and more efficient agricultural solutions in the face of climatic changes. While the internet of things, machine learning and artificial intelligence have the capacity to optimize food production [5], their application is economically and technologically constrained. In fact, too high start-up costs are cited as the main factor that prevents farmers in developing countries from deploying controlled environment agricultural systems [6].

Is it possible to build a low-tech high-performing hydroponic or aeroponic system?

In developing countries, low-tech hydroponic and aeroponic systems are more commonly adopted and structural components are substituted with locally accessible materials [7]. Even in such challenging conditions, and given financial constraints, further improvements to efficiency of farming is possible with better understanding

of flows and losses of heat, gasses, water and nutrients and optimisation of design of the low-tech hydroponic and aeroponic facilities in developing countries.

1.2 Black-Box Modeling

1.2.1 Fault Prediction Subsystem

A key challenge for low-tech controlled environment agriculture systems is effective control of the growing environment and the flows required to sustain the plants. Faults in the envelope of the growing module lead to losses of water, nutrients and an imbalance in ambient temperature. The black-box model of the desired fault detection system is shown in figure 1.1.

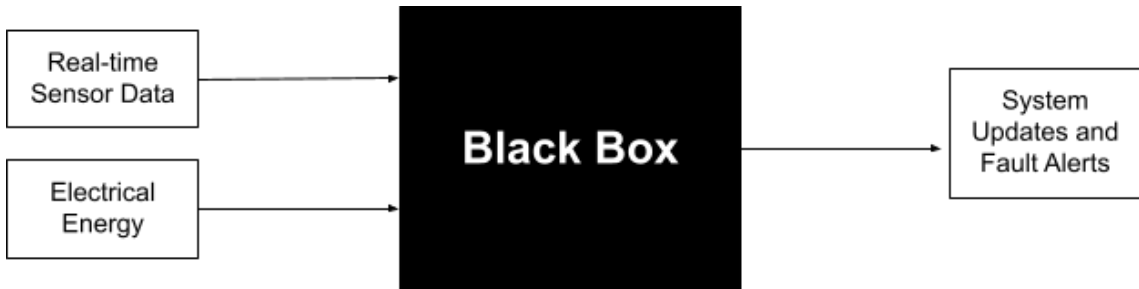


Figure 1.1: Black-box model of fault detection subsystem

In order to increase the accuracy and speed of fault detection in our aeroponics module, we plan to incorporate both steady-state and transient system analysis. To achieve steady state fault detection, we will create a heat-flow simulation of our system in MATLAB. By implementing the suggested design of the growing system in MATLAB, we will be able to quickly investigate the effect of changing parameters such as the thermal conductivity of the insulation material, the external temperature and the solar radiation intensity. We will also be able to generate equations based on a simplified setup and solve them analytically to determine acceptable sensor data ranges.

To provide transient analysis, we plan to implement our physical aeroponics system and record sensor data while the system is subject to various faults. For example, we will begin recording data and then create a hole in the insulation. As another example, we will begin recording data and then turn off the pump. We will use these time series datasets as the inputs to a supervised long short-term memory (LSTM) machine learning algorithm. This model will be trained to predict the time at which the faults occurred. Although the training process is computationally intensive, it only occurs once, offline. The model parameters can be copied and used in a lightweight program that can run on a board such as a RaspberryPi. As a result of the training process, the module will be able to predict major faults such as those described above before they cause the environmental variables to fall into a range that is inimical to plant survival. A detailed black-box model of the desired fault detection system that includes the steady-state simulation and transient analysis is shown in figure 1.2.

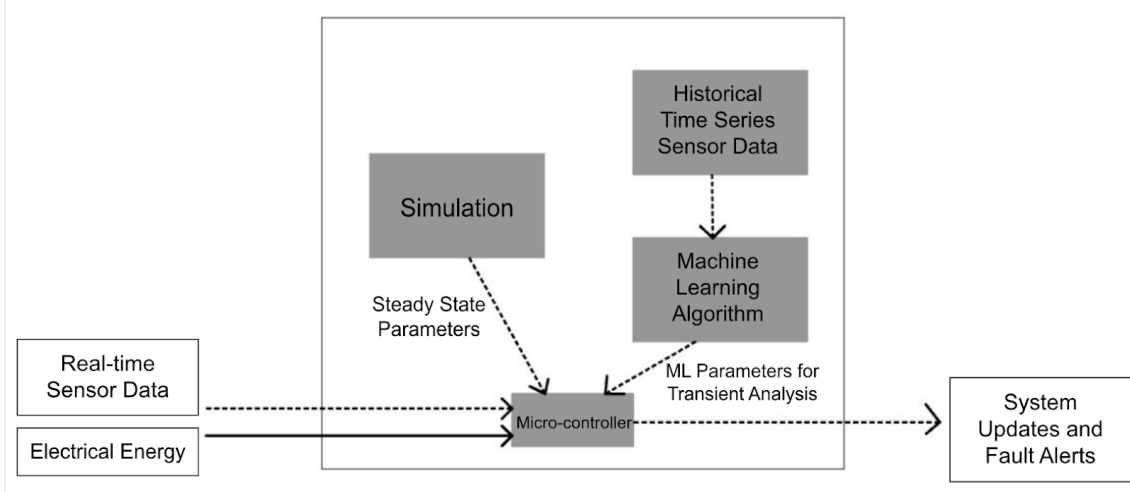


Figure 1.2: Elaborated black-box model of fault detection subsystem

1.2.2 Full Aeroponics System

The full aeroponics system takes only water, nutrients, sunlight and electrical energy as inputs, and outputs plant produce. In our case, the system also outputs digital information in the form of system updates and alerts. These inputs and outputs do not rely on human intervention in the case of normal operation and minor system disturbances, therefore minimizing the administrative burden on the user. Hence, the training required to operate the system is minimal. The water and nutrients are located in an actuated storage chamber, whose actuators (eg. pumps) are connected to the microcontroller. The microcontroller adds more nutrients/water to the solution pool according to its predetermined parameters and the readings from the EC, pH and temperature/humidity sensors. The system will also output error messages based on these sensor readings as well as the data from the light sensor. The solution is delivered to the plants via the pump, according to a timing schedule controlled by the microcontroller. Water usage, nutrient waste and electrical energy consumption are minimized as a result of the timed operation of the pump. A simplified black-box model of the system is shown in figure 1.3. A detailed black-box model of the system that includes electronic and agricultural system is shown in figure 1.4.

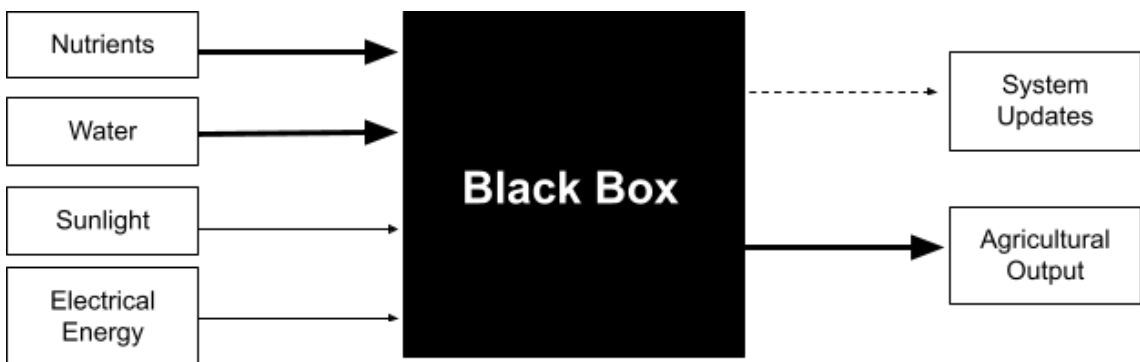


Figure 1.3: Black-box model of full aeroponics system

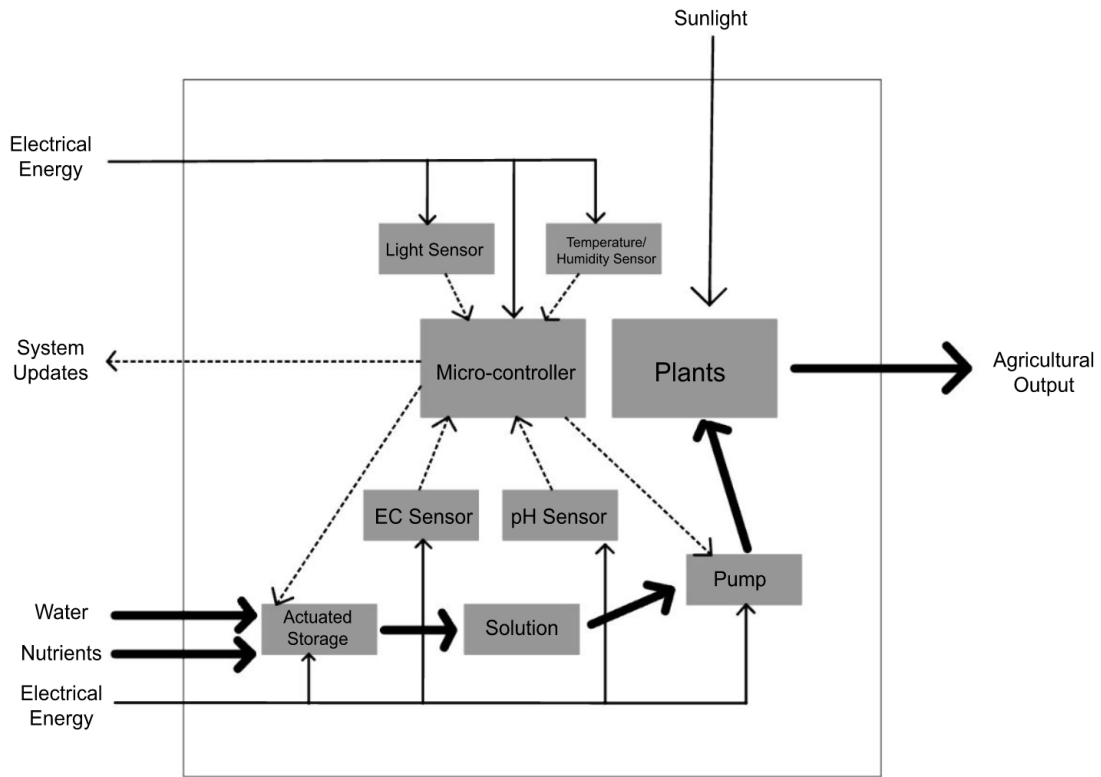


Figure 1.4: Elaborated black-box model of full-aeroponics system

1.3 Problem Statement

At present, setting up an aeroponics facility is capital-intensive and requires significant knowledge in the areas of engineering and agriculture. This makes designing aeroponics solutions for the developing world challenging, and explains the paucity of options that are available to farmers in such regions. We aim to increase the accessibility of aeroponics growing systems through the creation of a framework of open-source automated control systems and low-cost hardware, structural and hydraulic solutions. The constraints that frame this problem are primarily those faced by farmers with limited private or government backing in developing countries: low capital, intermittent power access, water scarcity and limited technical knowledge. These constraints are elaborated in section 1.4. Two open-ended questions stemming from this problem statement are included below:

1. To what extent do low-cost aeroponics systems require a controlled root-environment, present in high-cost systems, in order to maintain plant conditions within an acceptable range?
2. Can the use of sophisticated monitoring algorithms on real-time sensor data enable the root-environment to be maintained within acceptable limits while using lower-cost construction materials, by allowing the user to adapt more quickly to potential system faults?

The primary motivation of our project is to improve the accessibility of aeroponics, so an important outcome is to create resources that allow others to benefit from

the findings of our project. Therefore, we will produce well-documented design documents for all of our hardware (including technical drawings, circuit board files, fluidic circuit diagram) that minimize the effort required to recreate our system. Most importantly, we will release open source versions of the firmware and software that we develop for the automatic control and fault detection capabilities of our system. If we have time, we will also develop and release a web interface that allows users to easily monitor their system remotely.

1.4 Design Constraints

1.4.1 Technical Constraints

Structural integrity

There are constraints on structural integrity of the growing unit. The material, shape and size of the frame will have to be selected accordingly to withstand the weight of the mechanical and hydraulic components and the envelope. Analysis of structural components will be carried out to ensure sufficient strength of the structure. Vertical shear, bending moment, buckling and deflection will be considered. Minimization of material use is preferred to reduce the weight and size of the structure. The expected weight of the growing system (electrical components, plant support, plumbing; excluding the weight of the structural components) is 150 N when dry and 250 N when filled with water.

Thermal conductivity of the growing unit

Thermal conductivity of the growing unit is another constraint. Certain optimum conditions will have to be maintained inside the unit to provide a conducive growing environment and hence, the inside of the unit will have to be insulated from excessive influence from external weather conditions. The envelope will have to have appropriate thermal conductivity throughout its structure and also limit the exchange of water and water vapor between the inside and outside. The preferred thermal conductivity would be less than $0.03 \frac{W}{mK}$. This number is derived from [7], where polystyrene is recommended as the gold standard insulating material. According to [8], the thermal conductivity of expanded polystyrene when measured according to ISO 8301 standard is $0.03 \frac{W}{mK}$ at room temperature.

Temperature and Humidity

In order to maintain healthy plant growth, the root environment has to be maintained within certain levels. For potatoes, the temperature should not exceed 30°C and should ideally remain below 25°C for tuberisation [9]. The humidity should be in the range 80 to 90 percent in the root zone to ensure the roots do not dry out and to provide sufficient water for the whole plant [10].

Size

The size of the module is limited by its desired portability and modularity. This approach imposes a constraint on the implementation of the envelope. In real-world systems, many modules are packed closely together under a single envelope [11]. Additionally, in real-world applications in developing-countries we anticipate that

ground area will not be a significant design constraint as it is in highly-developed urban environments. Building a full system with many modules and a large envelope is beyond the scope of our project. Therefore, we aim to build a single module that is less than 1.5 m high with a base of 2 m x 1 m.

Electricity supply

Aeroponics relies heavily on constant power to keep plants alive. As we are designing our system to reduce scarcity in developing countries, we must ensure that it is resilient to power outages. We assume that power outages last on average 5 hours and occur daily. Given that an average solar system battery has capacity of 10 kWh, we set the maximum power demand to 1 kW to preserve a margin of safety. Otherwise, electricity from the grid would be available.

Internet connectivity

We must be able to alert the user to faults in their system immediately (within 30 seconds of fault detection). We assume that internet connectivity is as unreliable as the power. Specifically, we assume that the area has mobile service no better than 3G (which offers 3 Mbps) We also assume that the aeroponics facility manager has a smartphone on them at all times.

Water supply

We assume that there is a limited supply of sterile water close to the aeroponics facility. We make this assumption as it is beyond the scope of our project to design a water purification system. Given that existing aeroponics systems result in up to 95% water saving compared to irrigation agriculture [12], we aim to ensure that the daily water consumption of the facility is less than 5% of the amount of water required for the same crops grown in conventional farming systems. The specific water demand will be computed for each respective crop.

Nutrient supply

We assume that nutrients are accessible to the facility manager at standard international prices plus shipping. We make this assumption because it is beyond the scope of our project to investigate alternative sources for the nutrients. We believe this assumption is consistent with the assumption that there is sufficient capital and accessibility to set up the system. However, we aim to minimize the nutrient usage in accordance with other constraints such as cost.

1.4.2 Non-Technical Constraints

Growing capacity

We do not intend our system to replace traditional agriculture on the level of a subsistence farmer. We envisage our system as a tool for creating high quality produce in larger settlements (ie. settlements with stable power and mobile service). The aim of the system is to increase food supply by providing communities with better-performing growing system and by reducing the percentage that they have to obtain from water- and soil-intensive agriculture. Based on similar developed systems and described in the literature, for potato, the goal for the system is to produce 50 kg of potato per month [9].

Modularity

To meet the growing capacity requirements of our planned aeroponics facility, individual modules must be connected together. As mentioned above, we assume that ground area is not scarce. Therefore, we aim to design a planar system - modules are connected in the horizontal plane and are not stacked vertically as they are in high-tech systems in developed urban centers. A major advantage to this approach is that all plants can access natural lighting so energy costs related to lighting are eliminated.

We must also consider the modularity of the technological system. Each module would keep a constant temperature, so the temperature of each module must be monitored. However, the water can be shared between modules. Therefore, we should design our hydraulic system to connect directly to a pump, or to connect to another module on one or both sides. We must also design our circuit and software to receive information from as many temperature sensors as there are modules, but from single pH and EC sensors. Additionally, the software must be able to detect faults and generate alerts for each module in order to ensure the integrity of the entire aeroponics system and a high yield.

Finally, we should consider the accessibility of each module. At a minimum, the module must be accessible from one side. The configuration resulting from this requirement would be a doubly-lined row of modules. If accessibility is increased to two sides, the resulting configuration is a single row of modules.

Cost

The most important constraint for our project is the cost of the system. The cost can be broken down into two components: capital expenditure and running costs.

Capital expenditure includes the initial costs of purchasing the structural components, hydraulic components, doors, walls and insulation, and electronic components. Running costs include the cost of electricity, water, nutrients, seeds and repairs.

In order for our work to be applicable in the world, there are two cost constraints. Firstly, we want to make our system commercially competitive with aeroponic sets present on the market. The current price range is above 1,000 USD [13]. At the same time, we want to control for being competitive in the context of profitability of the produce. In the UAE, a kilogram of potatoes costs 3 AED. For a system that produces 50 kg of produce per month and the lifetime expectancy is at least 5 years, the expected revenue is 9,000 AED in real terms. Hence, the price ceiling of 1,000 USD is appropriate, especially after accounting for depreciation and labour. In fact, operators of aeroponic facilities can charge premium on their long-term contracts given the stability of supply.

Technical knowledge

We assume that the facility manager has experience using a smartphone. We also assume that they have no experience of aerponics or any of its subsystems.

Chapter 2

Conceptualization

2.1 Background Research

The field of aerponics has experienced two waves of technological innovation [14]. The first wave began in the 1960s with the inception of aerponics as a technique distinct from hydroponics, and continued until the late 1980s with the commercialization of the first closed-loop system controlled by a single microprocessor. This first wave of innovation occurred before the advent of the internet and powerful machine learning, and before the rise of mass-produced, low-cost LEDs. For this reason, the body of literature from this period does not leverage many of the important technologies that are available today and therefore has little bearing on our current project [15]–[17]. The second wave, which has occurred only within the last decade, attempts to improve on traditional aerponics techniques by incorporating the above technologies to increase the efficiency and improve the accessibility of the process. The body of literature from this second wave is thin and of mixed quality. There are three main reasons for this: the first, already mentioned, is that it is relatively nascent; the second is that much of the research has been carried out in the private sector and is not reflected in the scientific literature; the third is that public research in this area is predominantly conducted in developing countries with limited resources and subsequently published in second-tier journals.

[18] is a comprehensive review of the developments in aerponics in recent years. It is a useful resource presenting us with the choices we had to make regarding pumps and nozzles, and by providing guiding values for EC, pH and interval timings.

There has also been advancement in the use of artificial intelligence and other advanced technologies in optimizing the use of aerponics. [19] investigated the thermal and morphometric characteristics of lettuce grown in an aeroponic system through a computer vision technique based on multispectral images. In this paper, images of the roots and leaves were captured with near infra-red (IR), far IR and visible light spectrums. These images were processed using handcrafted MATLAB algorithms, and were used to estimate the root and leaf area, perimeter and length for each plant. They did not use any machine learning techniques.

[20] demonstrated the use of sensor readings combined with analytic formulae to reduce plant disease. They measured environmental conditions within a greenhouse

and implemented a control system to ensure that the dew point of the leaves is not reached. The system was composed of relay nodes which receive sensor readings, send them to a server, and run commands to control devices such as ventilation fans, windows and internal circulating fans. This paper demonstrates the modularity in control that we wish to achieve in our project.

[21] explored the use of control algorithms based on machine learning and modular sensor systems in the context of aeroponics within a greenhouse. The paper describes a system of remote modules that can send sensor data to a central fault detection system and receive feedback in response. Unfortunately, the paper is largely theoretical and no further research was produced by its authors.

[22] investigated the ability of a neural network to detect mechanical (sensor or actuator) faults and biological faults. They found that they were able to detect mechanical faults within an hour on average. However, the output of their model was a single ‘faulty’ signal that did not distinguish the type of mechanical fault (eg. pump, nutrient control, temperature sensor, pH sensor). This places a large educational burden on the operator, as they are required to diagnose the problem once they have been alerted to it. The authors also found that they were unable to detect biological faults. The models used in this paper take only two sensor readings (corresponding to t and t-1) as inputs, significantly decreasing their predictive power.

[23] developed a sensory platform specifically for commercial aeroponics. It consists of light, pH, temperature and electrical conductivity sensors, as well as a radio communication module. This platform contains all of the functionality that we wish to implement, with the exception of humidity and gas concentration measurement. In conclusion, the latest literature points towards development of modular aeroponic systems that implement machine learning, image recognition and real-time monitoring to improve the efficiency of growing. In the present work, we aim to further investigate and advance this trend.

2.2 Concept Generation

Based on the possible variants of the design of the growing system, three main variable components of the design are considered. The three considered variables are:

- Type of growing technology
- Type of growing structure
- Type of environmental control

Firstly, the **type of growing technology** may be either aeroponics, hydroponics, fogponics or aquaponics [18]. Hydroponics stands for a soilless growing system where the medium of delivering nutrients is standing or flowing water. In aeroponics, nutrients are delivered through droplets of water. In fogponics, nutrients are delivered through smaller water droplets that are on the same size scale as fog. The final option is aquaponics which works like hydroponics but the source of nutrients

is a tank with fish rather than artificial injection of chemicals.

The second variable is the **type of growing structure**. In the first variant, the plants would be grown in open air. In the second type, the plants would be grown in open air but separated by a net that prevents interference by birds and excessive access of insects. The remaining two variants utilize an indoor growing environment. The first alternative is using an opaque envelope with no access to natural light. The second alternative is a translucent envelope that allows for access to natural light.

The third variable is the **type of environment control**. In the first variant, there would be no control of the growing environment and it would be fully dependent on the atmospheric conditions, including temperature, light and humidity. In the semi-controlled environment, the system would control the key variables such as lighting or excessive fluctuations of temperature through simple electronic components such as fans or lights. In the third variant, there would be a high-tech control system of the indoor environment, monitoring light, temperature and humidity and applying appropriate responses to keep the growing conditions within designated bounds.

To evaluate the viability of the considered variants listed above, morphological chart and pugh chart methods are used. The morphological chart with a list of considered options for the growing unit design are shown in table 2.1.

Table 2.1: Morphological chart for growing unit design

Means	Growing technology	Type of growing structure	Type of environment control
1	Aeroponics	Open-air	No control
2	Hydroponics	Open-air, separated by a net	Partial control (fan/lights)
3	Fogponics	Indoor, opaque	Full control (air conditioning, lights, air (de)humidifier)
4	Aquaponics	Indoor, translucent	

2.3 Concept Selection

As the next step in the concept selection process, the pugh chart is implemented to compare different options. We will be testing the different types of growing structures to find the most optimal design for our system. Our system would be a low-tech system that can be easily applicable in developing countries, which causes us to drift away from a fully-controlled environment while still trying to create an environment that maintains plant conditions within an acceptable range.

In order to choose a growing technology, we compared the four options at hand with criteria that represent our priorities in this project. The criteria are:

- Learning opportunity

- Impact on society
- Applicability using low-cost materials
- Existence of previous research
- Intellectual property opportunity
- Saturation of market

Our most important criteria is the learning opportunity that exists from investigating this growing technology. Other important factors include the applicability of the growing technology using low-cost materials as this would be our main approach to this project, in addition to the impact our design can have on the society especially in developing countries, where this solution would generate benefits for the local communities. The amount of research previously done on the technology is also of importance, as we are looking to investigate issues that have not been deeply researched yet. The saturation of the use of the technology in the market was also considered, however, it was not of great importance, as we are more keen to learn and to benefit others rather than creating a product that would sell. We also considered the opportunity of pursuing intellectual property for our design, which we know can be a challenge regardless of the growing technology we choose.

Weighted Pugh charts were developed with the criteria mentioned above to assist us with the selection of the growing technology, the type of growing structure and the type of environment control that we will be using. As an example, consideration of the type of growing technology is shown in the following figures. Figures 2.2, 2.3, 2.4 and 2.5 show the pugh charts with aeroponics, hydroponics, fogponics and aquaponics as the base of evaluation, respectively.

Table 2.2: Pugh chart for growing technology with aeroponics as the base

Concept	Learning opportunity	Impact on society	Applicability using low-cost materials	Amount of research previously done	IP opportunity	Saturation of market	Sum	Rank
Relative Order	0.25	0.225	0.225	0.15	0.10	0.05		
Aeroponics	B	A	S	E			0	1
Hydroponics	0	0	0	-1.00	0	-1.00	-0.20	2
Fogponics	0	-1.00	0	0	0	0	-0.225	3
Aquaponics	0	-1.00	0	0	0	0	-0.225	3

Based on the results of the pugh charts given the selected criteria and their assigned weights, we chose **aeroponics** to be the growing technology that we will be investigating in our project. The Pugh charts above show that aeroponics satisfies the chosen criteria the most in comparison to the other growing technologies. Analogous analyses are performed for the type of growing structure and the type of environment control. **Open-air, separated by net** growing structure and **partial control (fan/lights)** environment control were selected for this project.

Table 2.3: Pugh chart for growing technology with hydroponics as the base

Concept	Learning opportunity	Impact on society	Applicability using low-cost materials	Amount of research previously done	IP opportunity	Saturation of market	Sum	Rank
Relative Order	0.25	0.225	0.225	0.15	0.10	0.05		
Aeroponics	0	0	0	+1.00	0	+1.00	0.20	1
Hydroponics	B	A	S	E			0	2
Fogponics	0	-1.00	0	0	0	+1.00	-0.175	3
Aquaponics	0	-1.00	0	0	0	+1.00	-0.175	3

Table 2.4: Pugh chart for growing technology with fogponics as the base

Concept	Learning opportunity	Impact on society	Applicability using low-cost materials	Amount of research previously done	IP opportunity	Saturation of market	Sum	Rank
Relative Order	0.25	0.225	0.225	0.15	0.10	0.05		
Aeroponics	0	+1.00	0	0	0	0	0.225	1
Hydroponics	0	+1.00	0	-1.00	0	-1.00	0.025	2
Fogponics	B	A	S	E			0	3
Aquaponics	0	0	0	0	0	0	0	3

Table 2.5: Pugh chart for growing technology with aquaponics as the base

Concept	Learning opportunity	Impact on society	Applicability using low-cost materials	Amount of research previously done	IP opportunity	Saturation of market	Sum	Rank
Relative Order	0.25	0.225	0.225	0.15	0.10	0.05		
Aeroponics	0	+1.00	0	0	0	0	0.225	1
Hydroponics	0	+1.00	0	-1.00	0	-1.00	0.025	2
Fogponics	0	0	0	0	0	0	0	3
Aquaponics	B	A	S	E			0	3

Chapter 3

Modeling, Simulation and Optimization Plan

3.1 Modeling Results

The flowchart that outlines the iterative process for design of the aeroponic system in this project is shown in figure 3.1. The process entailed creating 3D models of the system, analysing the structural strength and thermal balance. If the designed system did not meet the constraints, the process was repeated. Eventually, the desired design was manufactured and assembled. In the process, industry experts were consulted on best practices for design and implementation. Once the system was operational, tests were performed and data was collected.

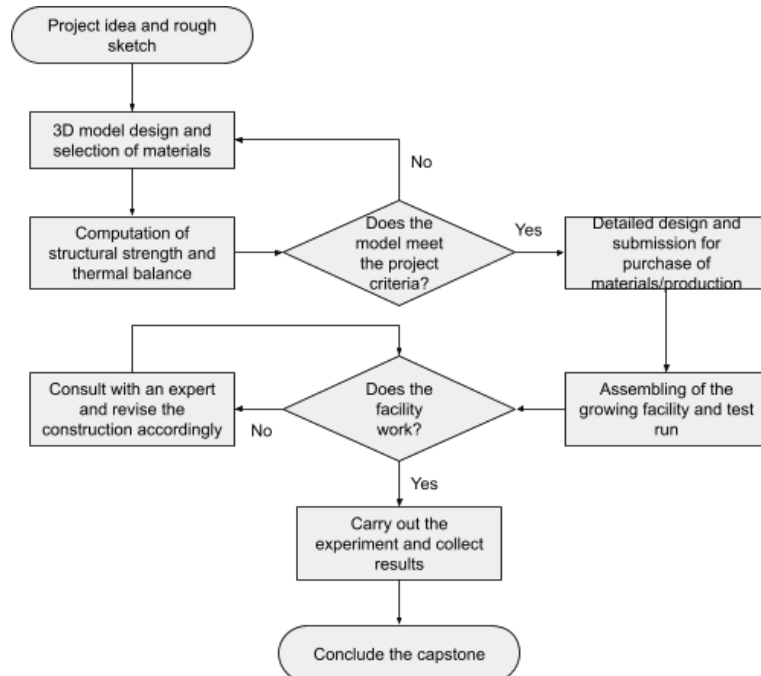


Figure 3.1: Flowchart for iterative design of the growing facility

3.1.1 Structural Subsystem

Based on the outcome of the conceptualisation process outlined in section 2.3, modeling of our project started with ideation of the structural subsystem and a rough sketch. Technical and non-technical constraints were considered in the process, as per specifications given in section 1.4. Then, a three-dimensional model, including the shape and the preferred materials, was created in Solidworks. The strength of the structure was computed using structural engineering techniques (SAP2000 software was utilized). The preferred material for manufacturing of the structural system was timber given its availability in the developing countries where the product is meant to be implemented. Timber is also relatively cheap and has sufficient strength.

The initial structural system was two 1 m x 1 m x 1 m timber cubes with plywood walls and supported on wheels or legs at the four corners. Structural analysis for the suggested design was performed using SAP 2000 in order to identify the most economic and efficient material use. The 3D model of the design was implemented in SAP 2000 with relevant loads applied, as shown in figure 3.2. Given that timber is not available in SAP2000, it is implemented manually with the following specifications: $\rho_{timber} = 450kg/m^3$, $E = 9GPa$ ($\rho_{al} = 2700kg/m^3$). The material used for walls is poplar plywood which is also inputted manually in the form of distributed loads ($\rho_{plywood} = 560kg/m^3$, $t = 0.015m$, not directly implemented in SAP 2000).

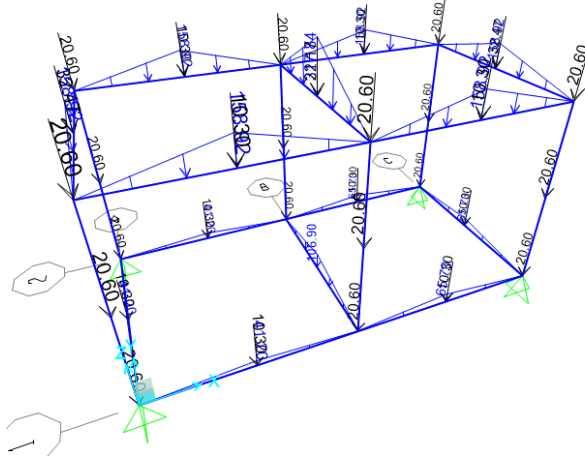


Figure 3.2: 3D model of the module in SAP 2000 with applied loads for 3 x 3 timber beams scenario

The structural loads that contribute to the total load are:

- Triangular distributed loads due to plywood on the upper grid and the lower grid of beams: $w_{max,plywood} = w_{plywood} \frac{L}{2} = 560 * 9.81 * 0.015 * 1 * 0.5 = 41.2N$
- Point load at each of the 8 points where the plywood walls of the module are pinned to the beams and columns: $P_{walls} = w_{plywood} * A * \frac{1}{8} = 560 * 9.81 * 1 * 0.015 * 0.125 = 10.3N$
- Own weight of the beam/column (computed by SAP 2000, not shown in the figure)

Additionally, non-structural loads due to the hydraulic system and plants were considered:

- Load due to the water tank placed inside the module modelled as triangular load on one of the square set of bottom beams (total mass of the tank and water of 5 kg is anticipated): $w_{max,tank} = w_{tank} \frac{L}{2} = \frac{5*9.81}{1} * 1 * 0.5 = 24.5N$
- Load due to the suspended beam holding the water pipe with nebulizers modelled as point loads on the upper beams: $P_{beam} + P_{pipe} = \frac{1}{3}(w_{beam} + w_{pipe}) = \frac{1}{3}(2700 * 7 * 10^{-4} * 2 * 9.81 + 3 * 9.81) = 22.17N$
- Load due to plants suspended in the upper layer of plywood modelled as triangular loads on the upper grid of beams: $w_{max,plants} = w_{plants} \frac{L}{2} = 24 * 9.81 * 0.5 = 117.72N$

Initially, the frame cross-section was set to be a 3 cm x 3 cm square. All beams and columns were set to have the same cross-section. The resulting vertical shear distribution is shown in figure 3.3. The greatest shear, moment, and deflection is experienced in the 2-meter lower beam. The greatest axial load (not shown in this figure) is experienced in the two central vertical beams. To ensure structural integrity of the system, the maximum shear stress, maximum bending stress and maximum deflection were considered for the horizontal beams. The maximum axial loads were considered for the vertical columns. In this design, the maximum shear is $V_{max} = 184.44N$, the maximum bending moment is $M_{max} = 160.87Nm$ and the maximum deflection is $d_{max} = 0.092m$. The distribution of vertical shear is shown in figure 3.3.

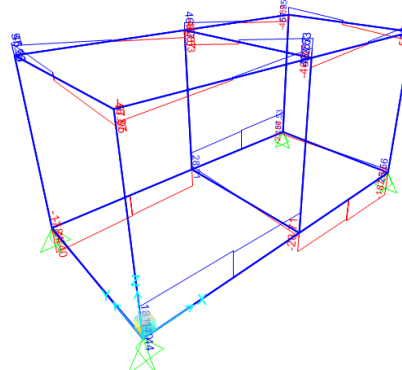


Figure 3.3: Shear 3D diagram for 4x4 timber structural system

The cross-sectional area of the square section is $A_{timber,1} = 0.03^2 = 9 * 10^{-4}m^3$ and the second moment of area about the y-axis is $I_{timber,1} = \frac{ab^3}{12} = \frac{0.03^4}{12} = 6.75 * 10^{-8}m^4$. Hence, the maximum shear stress and maximum bending moment are computed:

$$\begin{aligned}\tau_{max} &= \frac{V_{max}}{A} = \frac{184.44}{9 * 10^{-4}} = 0.205MPa \\ \sigma_{b,max} &= -\frac{My}{I} = -\frac{160.87 * 0.015}{6.75 * 10^{-8}} = -35.74MPa\end{aligned}\tag{3.1}$$

This design does not meet the design criteria as the maximum allowable shear stress for timber is typically 1 MPa and maximum allowable bending stress is 9 MPa.

Additionally, the vertical deflection of the beam of 0.092 m exceeds the maximum allowable deflection of 0.03 m. Hence, further optimization was performed to find a design that meets the selected constraints.

3.1.2 Hydraulic Subsystem

According to the initial design of the hydraulic subsystem, which consists of a 396 gallons per hour (GPH) pump submerged in the nutrient solution, leading the water into a 85 cm pipe placed vertically that is connected to a 1.8 m pipe placed horizontally with 24 nozzles and a blocked end, the velocity of the solution as it exits the nozzles is calculated using the volumetric flow rate of the solution and the cross-sectional area of the nozzles to ensure that the droplets reach the roots. The droplets are then traced to determine their trajectory to confirm that the droplets will intersect with the roots.

Performing a mass flow analysis is an essential step in ensuring the success of the hydraulics system for delivering water to the plants. To do this, we will need to gather information about the system's components, such as the pump, hoses, pipes, and nozzles. We will use this information to calculate the mass flow rate of the water solution as it travels through the system. This analysis will help us determine if the pump is powerful enough to deliver the required flow rate to the plants and if the nozzles are correctly sized and positioned to provide adequate coverage. By performing a mass flow analysis and performing necessary calculations, we can ensure that the hydraulics system delivers the water solution effectively to the plants, promoting healthy growth and optimal yields.

To perform a mass flow analysis for the given hydraulic system, we need to calculate the flow rate of the solution (which we will treat as water in this section for simplification) through the system. First, let's calculate the pressure head at the outlet of the pump. We know that the tank is placed at $h_1 = 10\text{cm}$ above the ground, the solution travels $h_2 = 85\text{cm}$ upwards, the pressure at the inlet of the pipe is $h_3 = h_2$ (equal to pressure at the top of the plastic hose) and pressure at the outlet of the pipe is equal to atmospheric pressure $h_4 = 0$. The total pressure head at the outlet of the pump is:

$$h_{total} = h_1 + h_2 + h_3 + h_4 = 10 + 85 + 85 + 0 = 180\text{cm} \quad (3.2)$$

Velocity of the water solution through the pipe is calculated using Bernoulli's equation:

$$\frac{\rho_1}{\rho} + \frac{v_1^2}{2g} + h_1 = \frac{\rho_2}{\rho} + \frac{v_2^2}{2g} + h_2 \quad (3.3)$$

Where ρ_1 is pressure at the inlet of the pipe, ρ_2 is pressure at the outlet of the pipe, ρ is solution density, v_1 is solution density at the inlet, v_2 is solution density at the outlet and g is gravitational acceleration. Assuming that the flow is steady and the pipe is horizontal, we can simplify the equation to:

$$v_2 = \sqrt{2gh_{total}} \quad (3.4)$$

Hence

$$v_2 = \sqrt{2 * 9.81 * 1.8} = 5.94 \text{ m/s} \quad (3.5)$$

Now, we can calculate the mass flow rate of the water solution through the pipe. The mass flow rate is given by:

$$\dot{m} = \rho A v \quad (3.6)$$

Where A is cross-sectional area of the pipe ($\pi r^2 = 0.000127 \text{ m}^2$). Hence

$$\dot{m} = 1000 * 0.0000127 * 5.94 = 0.75 \text{ kg/s} \quad (3.7)$$

Finally, we need to calculate the mass flow rate through each nozzle. There are 24 nozzles in the pipe, and each pair of nozzles is separated by 15 cm. Therefore, the mass flow rate through each pair of nozzles is:

$$\dot{m}_{nozzle} = \frac{\dot{m}}{12} = 0.063 \text{ kg/s} \quad (3.8)$$

Note that the flow rate through each nozzle is assumed to be the same, which may not be entirely accurate in practice.

To calculate the distance the water will travel after it goes out of the nozzle, we can use the conservation of energy again, but this time we will also take into account the losses due to friction in the pipe and the nozzle.

Assuming that the flow is turbulent, we can use the Darcy-Weisbach equation to estimate the pressure drop due to friction ΔP :

$$\Delta P = f \frac{L}{D} \frac{\rho}{2} v^2 \quad (3.9)$$

Where f is Darcy friction factor (assumed to be 0.02 for turbulent flow), L is length of the pipe, D is diameter of the pipe (0.0127 m) and v is velocity of the water through the nozzle ($Q/A = \frac{0.063/1000}{\pi * 0.0125^2 / 4} = 0.51 \text{ m/s}$, where Q is the volumetric flow rate per nozzle). Plugging in the values, we get:

$$\Delta P = 0.02 * \frac{1.8}{0.0127} * \frac{1000}{2} * 0.51^2 = 368.6 \text{ Pa} \quad (3.10)$$

The pressure drop due to friction will cause a decrease in the velocity of the water, which will lead to a decrease in the kinetic energy of the water. We can calculate the distance the water will travel using the conservation of energy:

$$\frac{1}{2} m v^2 = mgh - \Delta PV \quad (3.11)$$

Where V is volume of the water in the pipe after the nozzle ($AL = (\pi/4)(0.0127)^2 * 1.8 = 0.000228 \text{ m}^3$). Solving for h , we get:

$$h = \frac{v^2}{2g} + \frac{\Delta PV}{mg} \quad (3.12)$$

Plugging in the values, we get:

$$h = \frac{0.51^2}{2 * 9.81} + \frac{368.6}{0.02 * 9.81} = 0.44m \quad (3.13)$$

Therefore, the water will travel a distance of 0.44 meters after it goes out of the nozzle before it drops below the level of the nozzles.

The calculated distance that the water will travel after it goes out of the nozzle is an estimate based on a number of assumptions, such as assuming turbulent flow and neglecting other sources of energy losses such as minor losses due to fittings and bends in the pipe and losses due to viscous effects. Additionally, the actual performance of the nozzles could differ from the theoretical calculation due to factors such as nozzle wear and variations in the pressure and flow rate of the water. Therefore, while the calculated value provides a reasonable estimate, it should be considered as an approximation and the actual distance that the water will travel may vary.

In addition to neglecting energy losses due to friction in the pipe and nozzle, the calculation also neglects the effects of air resistance and other factors such as the effects of turbulence in the flow. When the water exits the nozzle, it will experience resistance due to the air in the environment. This can cause the droplets to disperse and fall more quickly than predicted, leading to a shorter distance traveled before dropping below the level of the nozzles. The effects of turbulence in the flow can also cause the velocity of the water to vary, which can affect the distance the water travels. Therefore, while the calculation provides a reasonable estimate, it is important to keep in mind that there are other factors that may affect the actual distance traveled by the water droplets.

Although the calculated distance that the water will travel after it goes out of the nozzle may not be completely accurate due to neglected factors such as energy losses and air resistance, it still provides useful information for the design of the aeroponics system. The calculated distance suggests that the water droplets should be able to reach the furthest row of plants, which is 30 cm away from the nozzles. Therefore, the system should work to supply water to all the plants, assuming that the nozzles are distributing the water evenly and the flow rate is sufficient to maintain the desired moisture level in the root zone. However, it is important to monitor the system's performance and adjust it if necessary to ensure that all the plants receive adequate water and nutrients for optimal growth.

3.1.3 Thermodynamics

The constraints governing the thermodynamic design aspects are outlined in section 1.4. We assume that the maximum external ambient temperature that the module will be exposed to is 40°C, and we want to ensure that the internal temperature does not exceed 30°C. To model the heat transfer through an uninsulated wall of the module we implemented a finite difference numerical method and used it to determine the time at which the inner surface of the cladding would reach 25°C, the maximum temperature at which the roots can be kept indefinitely without negative

effects. Figure 3.4 shows the time at which a surface 12.5mm from the outer surface at 40°C reaches a temperature of 25°C. For this setup, the time is 555 seconds. The value for the thermal diffusivity of the plywood was obtained from the manufacturer.

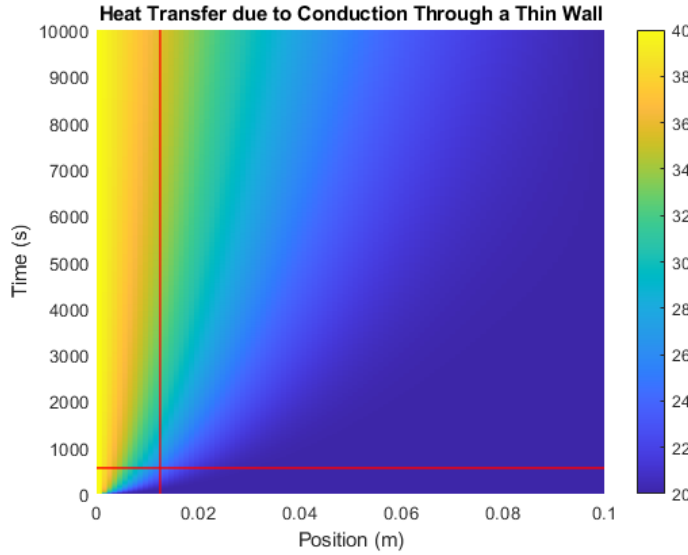


Figure 3.4: 1D heat transfer simulation through an uninsulated section of plywood cladding

To validate the efficacy of insulating the module with the polyurethane foam that was available from the NYUAD machine shop, we modified the simulation to include 25mm of foam before the plywood section. The thermal diffusivity of polyurethane foam used in simulation was obtained from [24]. The results are shown in Figure 3.5 below. Adding the foam insulation increased the time taken to reach the threshold temperature to 2600 seconds, more than five times greater than the uninsulated case.

To determine the effect of the plant holes on heat transfer through the top of the module, we modelled the top of the module as thermal resistors in parallel. To model the holes as high thermal conductors, we assumed that they were solid metal with a thermal conductivity comparable to copper. The thermal conductivity of the plywood was obtained from the manufacturer.

$$R_{\text{plywood}} = \frac{L}{k \cdot A} = \frac{0.0125}{0.1154 \times 1.906} = 0.05683 \text{ K/W}$$

$$R_{\text{holes}} = \frac{L}{k \cdot A} = \frac{0.0125}{500 \times 0.0942} = 2.65 \times 10^{-4} \text{ K/W}$$

$$R_{\text{total}} = \left(\frac{1}{R_{\text{plywood}}} + \frac{1}{R_{\text{holes}}} \right)^{-1} = 2.641 \times 10^{-4} \text{ K/W}$$

$$\dot{Q} = \frac{T_1 - T_2}{R_{\text{total}}} = \frac{40 - 25}{2.641 \times 10^{-4}} = 56800 \text{ W}$$

For holes with 5 cm diameter (corresponding to a design where the plants are mounted from the top of the module), the heat flow through the module was calculated to be 56800 W. This is extremely high and far beyond the capability of the

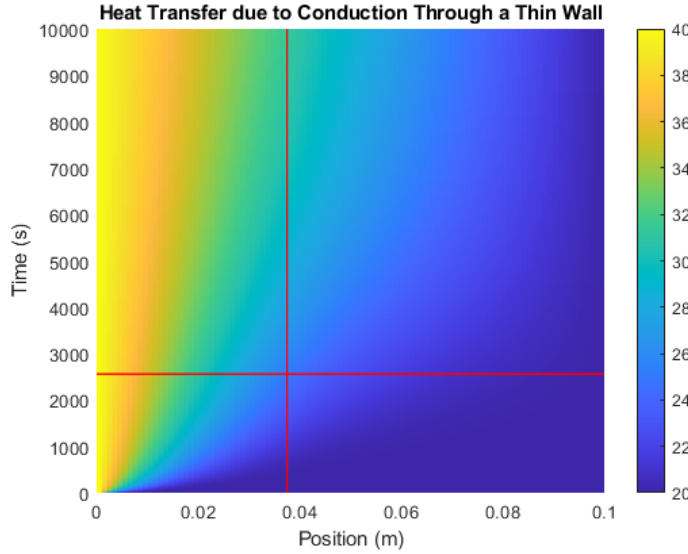


Figure 3.5: 1D heat transfer simulation through a section of the module wall insulated with polyurethane foam

module to cool itself. The improvements to this design are discussed in section 3.2.3 below.

3.1.4 Planting Subsystem

In this work, the main use of the plants is to quickly perform experiments and test the performance of the system in terms of thermal control, conservation of water and the functioning of software and electrical system. Furthermore, this project is in the field of engineering rather than agriculture so the selection of plants or their growing dynamics were not considered at this stage. The main consideration was for the planting subsystem at this stage was to have sufficient support system to keep the plants suspended in the structure. Simple commercial plant baskets are considered to be an appropriate solution in this case, as shown in figure 3.6. The completed setup with plant in the system would resemble the one shown in figure 3.7.



Figure 3.6: Example of plant well design in an aeroponic system [25]



Figure 3.7: Example of plant well distribution in an aeroponic system [7]

3.1.5 Electrical Subsystem

The power consumption of each component was calculated using ohms law based on the stated voltage input and current requirements in the technical data sheet. The modelled power consumption is shown in Table!?? below.

Item	Quantity	Current (mA)	Voltage (V)	Power (W)	Total Current (mA)	Total Power (W)
Main Pump	1	300	120	20	300	20
Nutrient Pump	2	40	120	3	80	6
AC Subtotal					380	26
Arduino	1	50	5	0.25	50	0.25
ESP32	1	250	3.3	0.825	250	0.825
Conductivity	1	6	3.3	0.0198	6	0.0198
PH	1	10	5	0.05	10	0.05
Light	1	0.02	5	0.0001	0.02	0.0001
CO2	1	125	5	0.625	125	0.625
O2	1	100	5	0.5	100	0.5
DC Subtotal					541.02	2.2699
Total					921.02	28.2699

The pumps consume 26kW while the microprocessors and sensors consume around 2.3W. Therefore, the system is modelled to consume a maximum of less than 30W when running. This is much less than 1kW, which is the limit identified in Section 1.4. Therefore, the modelling indicates that the electrical subsystem will adequately meet the design constraints.

3.1.6 Software

The maximum message size sent or received by the module is 128 bytes. Assuming a factor of 2 when including redundancy bits and other wrapping associated with messaging protocols, the total size of data transmitted is 256 bytes per message. Sending a message has a timeout of half a second before the transmission fails. The required bandwidth is therefore 0.5 Kbps as shown below.

$$\text{Bandwidth} = \frac{256 \text{ bytes}}{0.5s} = 512 \text{ bytes/s} \approx 0.5 \text{ Kbps}$$

This is three orders of magnitude less than the identified constraint for bandwidth identified in 1.4 so is very satisfactory.

3.2 Optimization Performed

3.2.1 Structural Subsystem

In the original modeling, the selected structural components were not sufficient to meet the design criteria in terms of maximum bending moment and deflection of the beams. In order to ensure sufficient structural strength of the growing module, further optimization was performed. The shape of the timber beams was varied in SAP2000 until satisfactory factor of safety was obtained. The previously identified design criteria of 1 MPa as the maximum allowable shear stress and 9 MPa as the maximum allowable bending stress were kept. Additionally, the maximum allowable deflection of 0.03 m was selected. Given the factor of safety of 1.2, the stresses should not exceed $\tau_{max} = 0.83MPa$ and $\sigma_{max} = 7.5MPa$. Deflection of the long beam should not exceed $d_{long,max} = 0.025m$. Deflection of the other beams should not exceed $d_{short,max} = 0.01m$. While it is desired to minimize the material use, it is not practical to have each beam and column with different dimension. Hence, we analyze two sets of beams: 2-meter beam in the bottom frame (which always experiences the greatest shear and moment) and the rest of the beams. For each set of beams, we consider different cross-sectional areas and the resulting maximum values of shear, moment and deflection to identify the optimum shape.

Firstly, the dimensions of the short beams are optimized. Dimensions of 2 x 2, 3 x 3 and 4 x 4 (all cm) are considered. The results of the simulations are shown in table 3.1. The V_{max} , M_{max} and d_{max} values are obtained from the simulation. The maximum shear stress and bending stress are computed analogously to computations in subsection 3.1.1. The 3 x 3 cross-sectional area is selected as the optimum design given that it meets the design criteria but it does not result in excessive material use.

Table 3.1: Optimization of dimensions of short beams

Dimension	V_{max} [N]	τ_{max} [MPa]	M_{max} [Nm]	σ_{max} [MPa]	d_{max} [m]
2 x 2	91.43	0.23	32.25	-24.19	0.022
3 x 3	92.53	0.10	32.53	-7.23	0.004
4 x 4	94.08	0.06	32.91	-3.09	0.001

After 3 x 3 cross-sectional area is confirmed as the dimension for the short beams, computation of stresses distribution in the long beams is performed to optimize their dimensions. The results of the simulation are shown in table 3.2. Based on optimization, a cross-sectional area of 5 x 5 (cm) is selected. This cross-sectional area is the smallest shape that meets the design criteria. The maximum bending stress slightly exceeds the desired maximum allowable bending stress of 9 MPa with factor of safety of 1.2 but given that this design does not result in any health or life hazards, this exception is permissible.

The final selection of cross-sectional areas for the structural sub-system is shown in

Table 3.2: Optimization of dimensions of long beams

Dimension	V_{max} [N]	τ_{max} [MPa]	M_{max} [Nm]	σ_{max} [MPa]	d_{max} [m]
3 x 3	184.44	0.20	160.87	-35.75	0.092
4 x 4	187.53	0.12	162.42	-15.23	0.029
5 x 5	191.50	0.08	164.40	-7.89	0.012
6 x 6	196.32	0.05	166.83	-4.63	0.006

figure 3.8. The distribution of vertical shear forces for the final design are shown in figure 3.9.

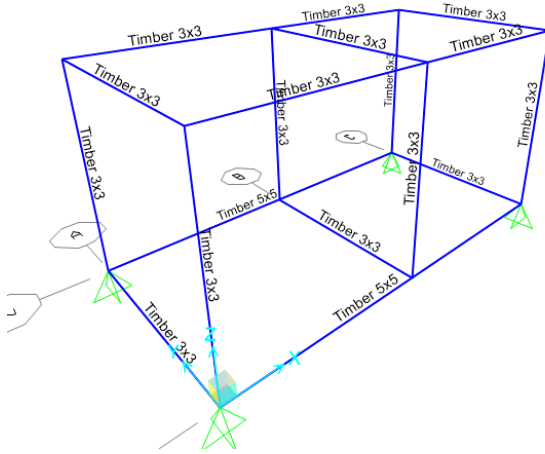


Figure 3.8: Assignment of the final frame section properties

3.2.2 Hydraulic Subsystem

No optimization was performed to the hydraulic subsystem at this stage, as the modelling calculations indicate that the design is sufficient to deliver the nutrient solution to the roots of all plants.

3.2.3 Thermodynamics

After considering the results of the initial thermodynamic modelling of the system, we modified how the plants would be mounted to the module. Rather than the plant basket resting on the outer surface of the top face of the module, which requires holes the same size as the basket, we mount the baskets to the interior ceiling of the module. In this way, the holes only need to be the same size as the plant stem. Updating the thermal resistivity network shows that the heat flow through the top surface is decreased to 4097W, more than an order of magnitude less than in the initial design. This is derived below.

$$R_{\text{plywood}} = \frac{L}{k \cdot A} = \frac{0.0125}{0.1154 \times 1.9936} = 0.5443 \text{ K/W}$$

$$R_{\text{holes}} = \frac{L}{k \cdot A} = \frac{0.0125}{500 \times 6.37 \times 10^{-3}} = 3.92 \times 10^{-3} \text{ K/W}$$

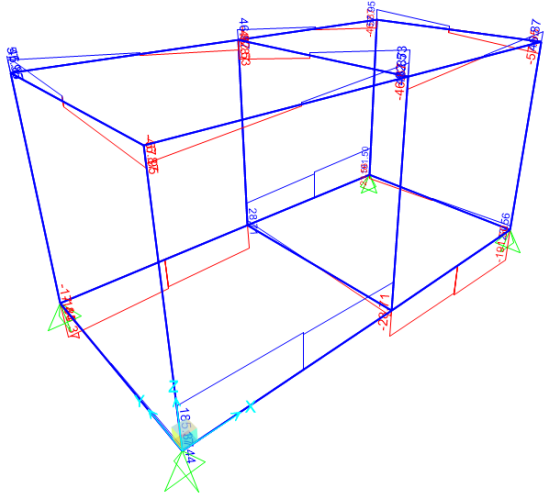


Figure 3.9: Distribution of vertical shear forces for the final timber design

$$R_{\text{total}} = \left(\frac{1}{R_{\text{plywood}}} + \frac{1}{R_{\text{holes}}} \right)^{-1} = 3.661 \times 10^{-3} \text{ K/W}$$

$$\dot{Q} = \frac{T_1 - T_2}{R_{\text{total}}} = \frac{40 - 25}{3.661 \times 10^{-3}} = 4097 \text{ W}$$

However, 4097W is still very large compared to the module's ability to cool itself. Without the addition of a cooling device inside the module, the only way for the module to cool itself is through evaporation of the water inside the tank. In this way, the remaining water will cool down and the air-water mixture in the module can then lose heat to the water to stay at thermodynamic equilibrium. The theoretical amount of water that would have to evaporate to achieve 4097W of cooling is derived below.

$$e_{heating} = c\Delta T = 4.18J/g \times (100 - 20)K = 334.4 \text{ J/g}$$

$$e_{state\ transition} = \delta H_{water} = 2260\text{ J/g}$$

$$e_{total} = e_{heating} + e_{state\ transition} = 2594.4\text{ J/g}$$

$$\dot{m} = \frac{W}{e} = \frac{4097J/s}{2260J/q} = 1.58 \text{ g/s}$$

Therefore, to balance the heat flow from the external environment 1.58g of water must evaporate every second. Not only is this impossible when considering that the air inside the module would quickly get saturated with water vapour and no more evaporation would be possible, but even assuming that it is possible it would result losing almost 6kg of water per hour.

To address this issue, we aimed to insulate the holes with rockwool. According to the manufacturer, rockwool has a thermal conductivity of 0.04 W/mK . The resistivity network values change as derived below.

$$R_{\text{plywood}} = \frac{L}{k \cdot A} = \frac{0.0125}{0.1154 \times 1.9936} = 0.5443 \text{ K/W}$$

$$R_{\text{holes}} = \frac{L}{k \cdot A} = \frac{0.0125}{0.04 \times 6.37 \times 10^{-3}} = 49.06 \text{ K/W}$$

$$R_{\text{total}} = \left(\frac{1}{R_{\text{plywood}}} + \frac{1}{R_{\text{holes}}} \right)^{-1} = 0.0544 \text{ K/W}$$

$$\dot{Q} = \frac{T_1 - T_2}{R_{\text{total}}} = \frac{40 - 25}{0.0544} = 276 \text{ W}$$

This results in a drop from 4097W to 276W when compared to the empty holes, more than an order of magnitude. Additionally, the water loss associated with the equivalent amount of evaporative cooling is 0.106g/s.

To further reduce the heat flow through the top plate, we take the above case and add 25mm of polyurethane foam insulation to the resistivity network. The effects on the heat transfer are derived below.

$$R_{\text{foam}} = \frac{L}{k \cdot A} = \frac{0.025}{0.025 \times 2} = 0.50 \text{ K/W}$$

$$R_{\text{total}} = R_{\text{holes}} + R_{\text{plywood}} + R_{\text{foam}} = 0.0544 + 0.50 = 0.5544 \text{ K/W}$$

$$\dot{Q} = \frac{T_1 - T_2}{R_{\text{total}}} = \frac{40 - 25}{0.5544} = 27.06 \text{ W}$$

Here, the heat flow through the system is again decreased by an order of magnitude when compared to the case where the holes are plugged with rockwool but the plywood is otherwise uninsulated. The water loss required to offset the energy influx associated with this heat flow is 0.010 g/s, meaning that it would take more than 26 hours to lose one kilogram of water due to cooling at this rate.

If the polyurethane foam is replaced with polystyrene (thermal conductivity of approximately 0.03 W/mK) the heat flow becomes 31.84W and the water loss due to evaporative cooling becomes 0.014 g/s. These values are within 15 percent of those for polyurethane foam, indicating that there is not a significant performance difference between the two.

To quantify the amount of evaporative cooling that is thermodynamically possible, we calculate the mass of water vapour in saturated air at 25°C as shown below where x is the mass ratio of water vapour to air in a saturated mixture at that temperature.

$$m_{\text{air}} = \rho_{\text{dry air}} \times V_{\text{interior}} = 1.293 \text{ kg/m}^3 \times 2 \text{ m}^3 = 2.586 \text{ kg}$$

$$m_{\text{water}} = m_{\text{air}} \times x = 2.586 \text{ kg} \times 20.0755 \text{ g/kg} = 51.9 \text{ g}$$

The energy required to evaporate 51.9g of water at 25°C is 135kJ, meaning that at the heat flow described in the insulated case it will take around 1.38 hours to go from dry air to fully saturated inside the module. After this time, in order for evaporative cooling to occur water vapour will have to be lost to the external environment (for example, by transpiration from the plant leaves).

3.2.4 Planting Subsystem

At this stage, there was no further optimization for setup of the planting system. As mentioned before, the purpose of this project is to optimize the control of the growing environment and optimize the design of the growing module rather than maximize the agricultural output as this subject is beyond the scope of this project.

3.2.5 Electrical Subsystem

No optimisation was performed on the electrical subsystem in response to the modelling results, as the model suggested that the power consumption of the system would be much less than the identified technical constraints.

3.2.6 Software

No optimisation needed to be performed on the software, as most of the design constraints associated with the software are not quantitative.

Chapter 4

Final Design

4.1 Initial Design Proposed

4.1.1 Structural Subsystem

Based on the optimization performed in subsection 3.2.1, timber beams and columns were found to be an appropriate material for constructing the growing module. The 3D view of the first design iteration created in Solidworks is shown in figure 4.1. The cross-section is shown in figure 4.2. The cross-sectional shape of the long beams in the lower frame is 5 cm x 5 cm and the cross-sectional shape of the other beams and of the columns is 3 cm x 3 cm. Figure 4.1 also shows the plywood walls and the wheels included in the growing module. Figure 4.2 shows the cross-section of the growing module design.

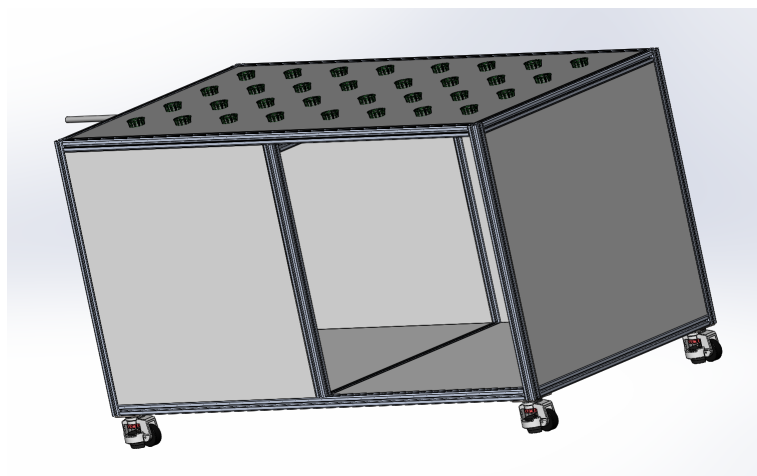


Figure 4.1: Three-dimensional view of the growing module design

4.1.2 Hydraulic Subsystem

The initial design of the hydraulic subsystem consists of a tank with a nutrient solution and a pump submerged in the solution to move the solution through a PVC pipe fitted to the pump and placed vertically. The vertical pipe is connected using an elbow fitting to a pipe placed and suspended horizontally, with nozzles to mist the nutrient solution on the roots, as shown in figure 4.3 done on SketchUp. A

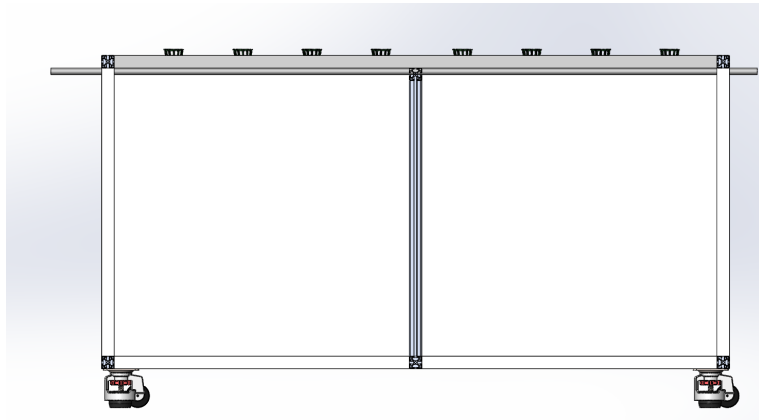


Figure 4.2: Cross section of the growing module design

layer of plastic sheeting will be placed under the pipe covering the whole area under the plants, and it is sloped with its end taped to the tank to drive the nutrient solution back into the tank.

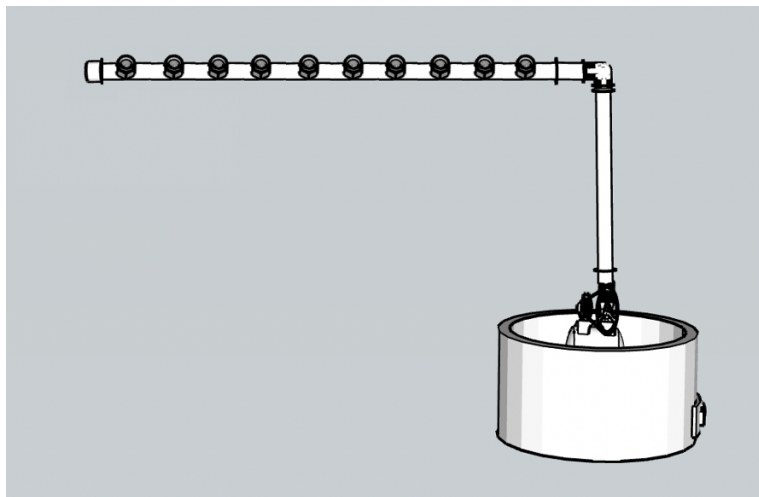


Figure 4.3: Initial design of hydraulics subsystem

The pump used in the system has a flow rate of 396 gallons per hour (GPH). The nutrient solution is pumped through a vertical pipe with a diameter of 0.5 inches, which is 85 cm long, and leads to a horizontal pipe with a diameter of 0.5 inches and a length of 1.8 meters. The pipe is suspended 95 cm above the ground and has 24 nozzles, each with a flow rate of 2 GPH.

The nozzles are placed at 12 equally-spaced marks along the pipe with a 15 cm separation between the marks and with two nozzles at each mark. The nozzles are oriented at an angle of 60 degrees toward each side. The roots of the plants are suspended 15 cm and 30 cm away from the pipe on both sides, and the system is designed to ensure that the droplets from the nozzles reach the roots.

4.1.3 Thermodynamics

When choosing the insulating material for our design, we wanted to minimise cost in line with the design constraints identified in section 1.4. After considering the results of the optimisation in subsection 3.1.3 polystyrene emerged as the ideal compromise between cost and thermal insulation. Sufficient polystyrene can be obtained from the supplier McMaster for \$185 as shown in Table 5.1, while the thermal conductivity is the same as that identified in the design constraints in section 1.4. Therefore, our initial design involves retrofitting 1" thick polystyrene to all faces except the bottom of the module.

4.1.4 Planting Subsystem

The grid of holes in the ceiling of the growing module can be seen in figure 4.1. The suggested grid of 4 x 8 wells has 32 growing slots. Given the growing area of 2 m^2 , this density is in line with growing densities found in the literature [7]. It is also expected to deliver the desired produce output of 50 kg per month. The growing system would make use of plant baskets shown in figure 3.6 that would be attached to the ceiling of the growing module on railings. Water and nutrients would be delivered through a hydraulic system described in detail in subsection ???. In the current design, the nutrient solution is carried by a single PVC pipe that runs along the bottom of the top surface. Nebulizers at fixed intervals along the pipe will transmit solution to the root zone in the form of a fine mist. The pipe is connected at one end to the pump, and has a cap at the other end. However, this cap can be removed so that the pipe from one module can be connected to that of another module, allowing the combined system to be powered from a single pump (of suitable power). The module has wheels so that it is portable.

The module will also have plastic linings on all interior surfaces and well as the exterior top surface (not shown). The interior will have black plastic to prevent light reaching the root zone and to ensure all nutrient solution returns to the tank and does not permeate the insulation. This lining will be fixed to the frame such that there is a gradient allowing gravity to draw the excess solution to a drainage pipe at the far end of the module. The external top surface will have a white plastic lining to reduce the absorptivity and limit the thermal load to the root zone.

The external structures are not shown in this diagram. An insect netting will surround the leaf environment, to minimize predation and reduce infection from various vectors of disease. Additionally, a shade cloth will cover a portion of the structure in order to further reduce the thermal load to the plants. This cover will be removable so that the plants receive the necessary light for photosynthesis even in low light conditions.

4.1.5 Electrical Subsystem

The initial design involved connecting the sensor array to an Arduino, which was then connected to an ESP32 chip to transmit data to the cloud. The pumps were purchased in the USA to run off 120V AC, while the sensors and micro-controllers operate at standard 5V or 3.3V DC. For full design and implementation details,

please see subsection 6.1.5.

4.1.6 Software

The constraints relating to the software subsystem are the internet connectivity and technical knowledge requirements. Specifically, the software should require bandwidth no less than 3Mbps and the system should be intuitive to use and require no configuration or error fixing. Figure 4.4 shows the initial software system design. In this system, the Arduino reads the sensors periodically and sends data to the ESP32 when the ESP32 sends a request. The ESP32 does this at fixed intervals and at the request of the user. The ESP32 connects to the internet through the nyuadguest network and establishes a connection with the AWS IoT servers. It then sends lightweight MQTT (Message Queuing Telemetry Transport) messages to the AWS servers. The user interacts with the system via the web application, which can be accessed on the internet. From the web application, the user can view historical data from the module and also send status requests to the module.

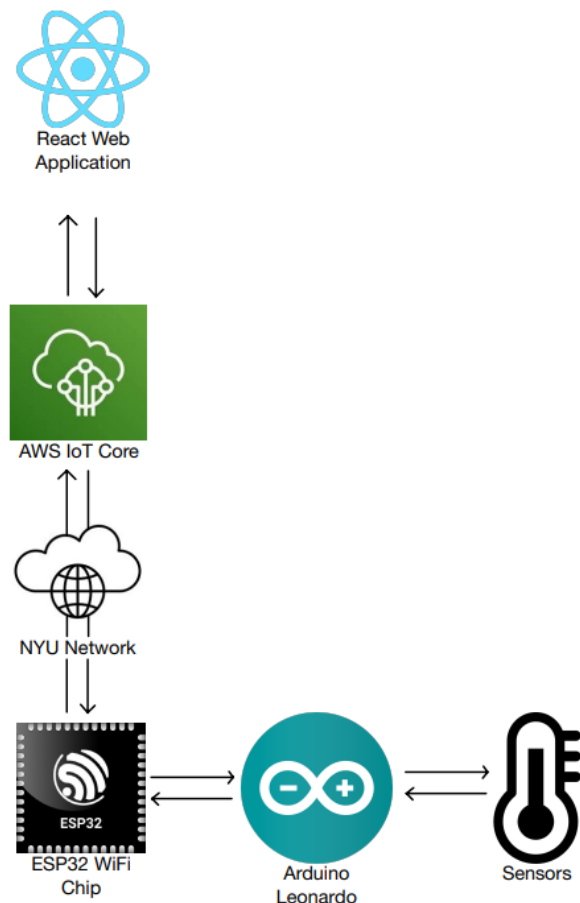


Figure 4.4: Data flow diagram of the initial software system design

4.2 Changes Made to Initial Design

4.2.1 Structural Subsystem

The selected material for design of the module was timber. However, based on the availability of tools and materials at NYU Abu Dhabi campus, aluminium frame was selected for building the prototype of the growing module. In order to ensure structural integrity of the design, structural analysis was performed. The materials used for this design are 6061 aluminum beams ($\rho_{al} = 2700kg/m^3$) and poplar plywood ($\rho_{plywood} = 560kg/m^3, t = 0.015m$, not directly implemented in SAP 2000). For aluminum beams, t-slot 4 x 4 cm beam that was available to us was considered ($A = 7 * 10^{-4}m^2$).

Analysis of the initial design indicates that the design is well within the constraints suggested by the design code. As for the previous designs, the structural component that experiences the greatest vertical shear, bending moment and deflection is the bottom beam on the longer side. For this component, the maximum shear is $V_{max} = 221.06N$, maximum bending moment is $M_{max} = 190.17Nm$ and maximum deflection is $d_{max} = 0.0065m$. As per the design analysis in SAP 2000, the design is well within the maximum allowable stresses for this material. The deflection is also acceptable for this project. The results of aluminium structure design check in SAP2000 are shown in figure 4.5. The values on the design check for each component vary from 0 to 1.0 and beyond, where value greater than 1 indicates that design code is violated. In fact, the selected material is extremely strong and would handle loads up to two orders of magnitude higher than what was expected for the growing module.

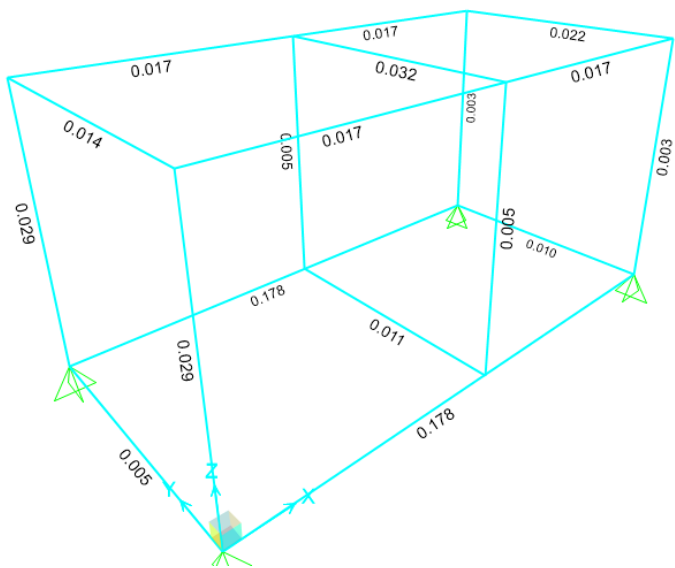


Figure 4.5: Aluminium structure design check

4.2.2 Hydraulic Subsystem

The initial design of the hydraulic subsystem underwent a change by replacing the 85 cm 0.5-inch pipe, positioned vertically, with a flexible 0.5-inch plastic hose. This

change was implemented to provide the flexibility needed to adjust the height of the horizontal pipe, making the model adaptable to growing various plant species with varying root lengths. By substituting the rigid pipe with a flexible hose, the system now allows for customization of the horizontal pipe's elevation depending on the length of the grown plants.

4.2.3 Thermodynamics

The selected material for insulating the aeroponic module was polystyrene, however this was unavailable from the NYU Abu Dhabi supplies. Instead, we used polyurethane foam. The analysis for this material is included in section 3.2.3. Polyurethane foam has a lower thermal conductivity compared to polystyrene so performs better as a thermal insulator, however, the difference is small (0.025 W/mK compared to 0.03 W/mK) so they are expected to give comparable performance. Therefore, to limit heat flow and retain moisture inside the module according to the technical constraints identified in section 1.4 we retrofitted 1" thick polyurethane foam on all faces of the module except the bottom.

4.2.4 Planting Subsystem

Traditional hydroponic and aeroponic setups involve placing plants in baskets and then placing the basket from above into a well above the water or mist. This requires the diameter of the well to be as large as the basket, which is significantly larger than the diameter of the plant's stem. Large holes such as these increase the effective thermal conductivity of the upper surface and compromise the module's ability to maintain a constant internal environment. To alleviate this issue, our design include half-inch diameter holes in the top surface with the intention that plants will be inserted and held from below. This change also allowed us to increase the density of plant wells from 4×8 (32 wells) to 4×12 (48 wells).

4.2.5 Electrical Subsystem

The initial design of the electrical subsystem did not include a switching mechanism for the pumps. This severely impacts the ability of the system to be used automatically, as it prevents the microcontroller from being able to activate the dosing pumps that modulate the pH and conductivity of the nutrient solution. In order to address this issue, we identified three design criteria for the switching mechanism as follows:

- Signals from the Arduino should be transmitted by a digital on/off signal
- One signal should control one pump, so three pumps require three signals
- The pumps should be able to be removed and reattached easily

These design criteria were supplied to Amjad Hamad in the ERB, who helped to design a switching board as shown below in Figure 4.6. This circuit board allows the pump wires to be reversibly attached to the switching board via FASTON tabs. This is convenient for assembly, disassembly and testing. Mechanical relays were used to implement the switching functionality, with digital signals from the Arduino

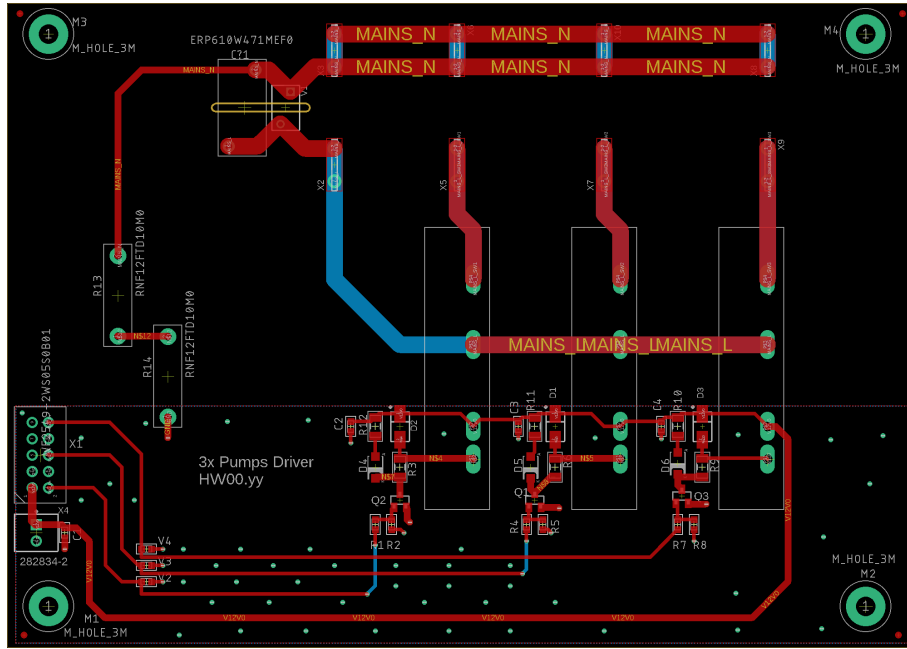


Figure 4.6: Layout of the pump driver PCB

controlling whether the relays were open or closed. The neutral phase of the AC mains power is common to all pumps, while the line phase is attached to the input of the relay. The line phase of the pumps is connected to the output of their respective relay. When the Arduino sends a signal, the circuit between the corresponding pump and the mains power closes and the pump switches on until the Arduino stops the signal.

4.2.6 Software

The initial design met the internet connectivity constraint as the system relied only on lightweight, MQTT messages, which can easily be received and transmitted over a network connection with a bandwidth less than 3Mbps. However, it does not meet the technical knowledge constraint as the user would have to provide AWS authentication from the command line. Additionally, as we began implementing the system we realised that we would need to integrate other AWS resources for storing data, sending timeseries data from AWS to the web application and managing user Authentication. The final system software design is shown in Figure 4.7 below. AWS Cognito is used to manage user authentication by routing new users through a log-in process. After logging in, all users can view historical data but only users who have been authenticated by us can send commands to the module. Historical data is stored in an AWS Timestream database, which is specifically designed for timeseries data. The incoming data from the module is automatically routed to the database via a function implemented in AWS IoT Core. To view the historical data, the web application makes an HTTP GET request to an AWS API connected to a Lambda function. This function queries the AWS Timestream table, returning the previous 24 hours of data.

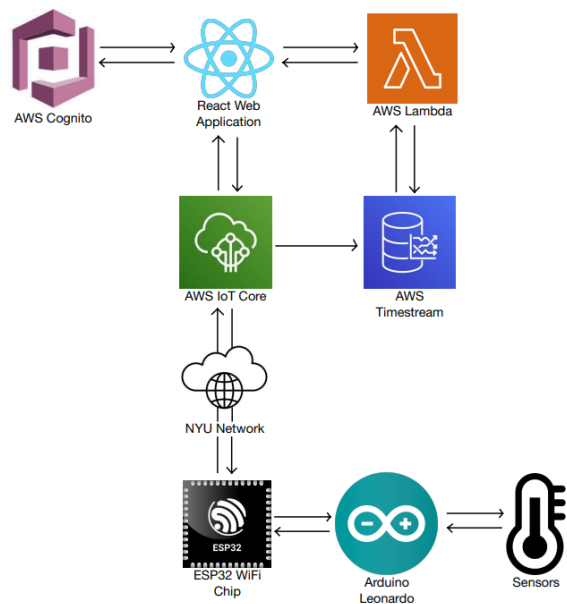


Figure 4.7: Data flow diagram of the final software system design

Chapter 5

Budget

Table 5.1: Budget for single module with materials as per preferred design

Item Name	Quantity	Cost/Unit (\$)	Cost (\$)
Main Pump	1	28.80	28.80
Conductivity Sensor	1	17.43	17.43
pH Sensor	1	34.99	34.99
PVC Elbow Joints 0.5in	1	0.93	0.93
PVC Pipe (5ft)	1	7.80	7.80
CDX 0.5" Grade Plywood Cladding (48" x 96")	6	30.75	184.05
Arduino Leonardo	1	25.00	25.00
ESP32 Development Board	1	6.00	6.00
Timber Framing (2" x 4" x 96")	8.2	5.79	47.48
Plastic Sheeting (24" x 45")	10	9.09	90.90
WiFi Antenna	1	5.00	5.00
Heavy Duty Velcro (1" x 20')	1	17.09	17.09
PVC Stop Valve	1	34.33	34.33
Temperature and Humidity Sensor	1	2.00	2.00
Breadboard wires	1	6.89	6.89
Plant wells	1	10.95	10.95
Misting Nozzles	1	59.00	59
Light Sensors	1	2.67	2.67
CO2 sensor	1	63.00	63.00
Oxygen Sensor	1	58.90	58.90
PermaProto Boards	1	8.33	8.33
Small Nutrient Pump	2	6.17	12.34
Polystyrene Insulation (6 pcs, 1" x 24" x 4')	2.2	85.00	187.00
Pump Driver Board	1	50.00	50.00
Total Cost			911.33

Table 5.1 gives the bill of materials for the construction of one module as per our final design. The quantities included in this table reflect the exact quantities used in one module, rather than the number we purchased. This means that the discounts

obtained by buying some items in bulk are reflected in the individual items above, which may not accurately depict the total capital required to build a single module. However, most of the items for which this is the case are the electronic components, such as the sensors and microchips. As discussed further in section 9.3, one major improvement to the module that we recommend is designing a custom circuit board. In this case the prices reflected above are accurate or even overstated, as the individual prices of electronic components are very low when purchased as part of a fabricated circuit board.

This budget additionally includes materials that are different than those we used to construct our module. The materials included above reflect those included in our final design, rather than the materials that we decided to use due to their accessibility to us on campus. The three major changes are the materials used for the framing (timber vs aluminium), cladding (CDX vs Marine grade plywood) and insulation (polystyrene vs foam). As discussed in section 4.2, these substitutions are justified based on the technical and non-technical design constraints.

Therefore, Table 5.1 gives an accurate depiction of the expected total cost of goods required to build one aeroponics module according to our final design.

Table 5.2 gives the bill of materials for the module that we constructed. As opposed to the budget in Table 5.1, this budget includes the total price paid for goods purchased in quantities greater than they were used in our design. It also includes the professional pH and conductivity probe that we used to calibrate and debug our system during the implementation and development process. Lastly, it includes the materials we actually used rather than those in our final design. It is mainly this last point that drives the cost of the module up much higher than in the budget in Table 5.1. We have included this higher budget to give transparency in the cost of developing our solution, however it does not accurately reflect the cost required to implement our final design.

Table 5.2: Budget for Module as Implemented

Item Name	Quantity	Cost/Unit (\$)	Cost (\$)
Main Pump	1	28.80	28.80
Conductivity Sensor	2	17.43	34.86
pH Sensor	2	34.99	69.98
PVC Elbow Joints 0.5in	15	0.93	13.95
PVC Pipe (5 ft)	1	7.80	7.80
Marine 0.5" Grade Plywood Cladding (48" x 96")	3	216.66	649.98
Arduino Leonardo	1	25.00	25.00
ESP32 Development Board	3	6.00	18.00
Aluminium Framing 40 mm x 40 mm x 10 ft	7	81.56	570.92
Plastic Sheeting (24" x 1')	10	13.75	137.50
WiFi Antenna	1	5.00	5.00
Heavy Duty Velcro (1" x 20')	1	17.09	17.09
PVC Stop Valve	1	34.33	34.33
Temperature and Humidity Sensor	5	2.00	10.00
Breadboard wires	1	6.89	6.89
Plant wells	1	10.95	10.95
Misting Nozzles	1	59.00	59.00
Light Sensors	3	2.67	8.01
CO2 sensor	1	63.00	63.00
Oxygen Sensor	1	58.90	58.90
PermaProto Boards	3	8.33	24.99
Small Nutrient Pump	3	6.17	18.51
Foam Insulation (54" x 1" x 1')	24	23.61	566.64
Professional pH and EC Probe	1	120.60	120.60
Pump Driver Board	1	50.00	50.00
Total Cost			2610.70

Chapter 6

Implementation

6.1 Report on Implementation

6.1.1 Structural Subsystem

The structural system as well as walls, floor and ceiling of the growing module were manufactured in the NYU Abu Dhabi Machine Shop. The structural components were manufactured using 4 cm x 4 cm T-slot 6061 aluminum. The installed walls, doors, ceiling and floor were made out of Korinplex poplar plywood with waterproof coating. The technical drawing submitted to the manufacturer is shown in figure 6.1. We keep in mind that, as the analysis above suggests, the use of weaker and less expensive materials should be sufficient for this structure.

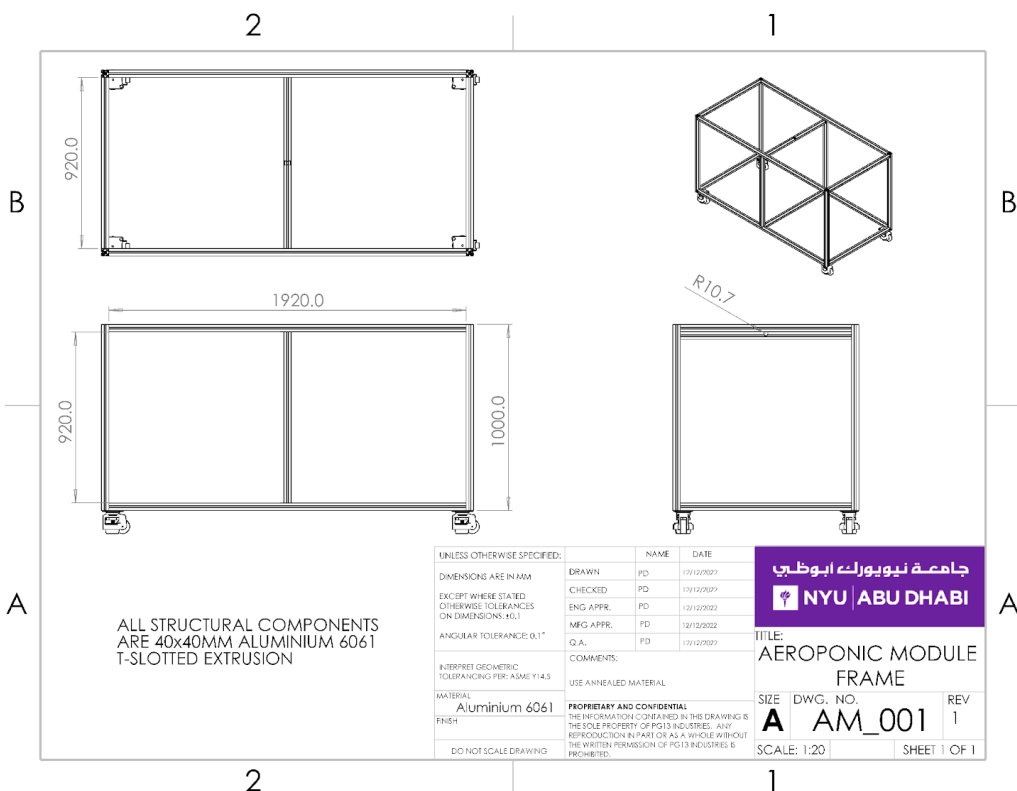


Figure 6.1: Technical drawing of the growing module

6.1.2 Hydraulic Subsystem

The hydraulic subsystem comprised a 5-gallon water tank, serving as the reservoir for the nutrient solution. Within the tank, the pump was positioned, submerged in the solution, to facilitate its movement. The plastic hose was securely fitted into the pump outlet, extending vertically from the tank. The hose was then connected to the horizontally placed pipe using an elbow fitting. The horizontal pipe, suspended from the aluminum frame at the top structure, featured strategically drilled holes to accommodate the placement of the 24 misting nozzles. Two nozzles were placed at each mark along the pipe, with a total of 12 marks and 15 cm separations between the marks. It was not possible to place 2 nozzles in one position as the diameter of the pipe was too small, so there was a 1 cm separation between every 2 adjacent nozzles.

The drain was constructed using a plastic sheet that was stuck to the roof of the model using duct tape. To make the drain sloped toward the tank, the sides of the sheet were stuck to the roof at a wide separation at the end of the pipe, with the separation getting narrower as the drain gets closer to the tank.

6.1.3 Thermodynamics

The polyurethane foam was attached to the top surface of the module as per the final design. However, there was not enough of this material in stock at the NYU Abu Dhabi campus to insulate all surfaces. Therefore, we had to conduct testing without insulation on all faces of the module, which significantly affected its ability to maintain a constant internal temperature. Additionally, the sealing tape ordered did not arrive so there were leaks at the interfaces between the module's faces.

6.1.4 Planting Subsystem

Four varieties of plants were tested in the growing system. Microgreens were selected given their faster growth rate compared to fully-sized varieties. By using microgreens, multiple trials could be conducted within the limited time available for testing of the system. The four species under consideration were kale, arugula, basil and tambay lettuce. Initially, the seeds were placed in rockwool plugs (1 inch x 1 inch surface area) and plants were left to germinate. The plants were watered manually in a tray (see figure 6.2). After five days, the germinating plants were transferred to the aeroponic setup. The watering system was turned on to periodically water the plants. Each trial run was expected to take 5 days for the plants to reach the maximum size.

6.1.5 Electrical Subsystem

The electrical system consists of three subsystems, namely the pumps, pump relays and microcontrollers/sensors.

The pumps were purchased from the USA, so they run off 120V AC power at 60Hz. In order to convert local 230V 50Hz AC power to meet these requirements, we purchased a transformer. The output of the transformer is connected to the pump



Figure 6.2: Germinating plants

driver board, which powers the pumps via relays. These relays operate at 12V and are powered from an external power supply connected to local mains voltage. The microcontroller and sensors operate at either 5V or 3.3V, but all are integrated into breakout boards that include voltage regulators so that a 5V supply is used for all of them. A 110/230V AC to 5V DC converter is used to power this subsystem.

All of the electrical connections between sensors, boards and pumps are shown below in figure 6.3. Red traces indicate positive DC voltage or the line wire for AC power. Black traces indicate ground for DC power and the neutral wire for AC power. Orange traces indicate digital signals, green traces indicate analog signals and blue traces denote serial connections.

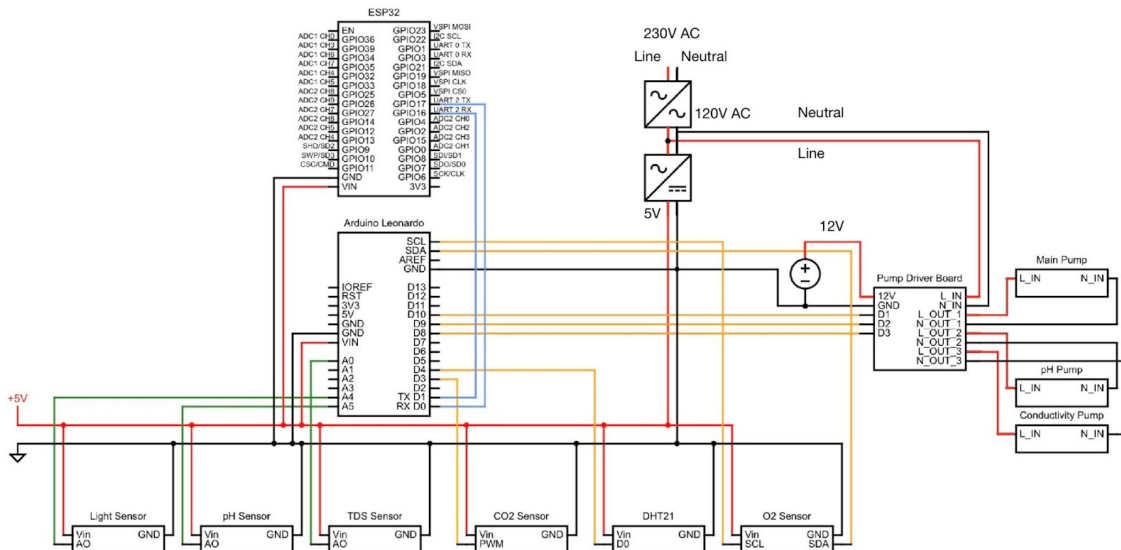


Figure 6.3: Electrical circuit scheme for the growing module

6.1.6 Software

Front end design: The most important design factors for the front-end software were ease-of-use and simplicity. To build a web application based on these factors, we created a single page design using the software Figma.

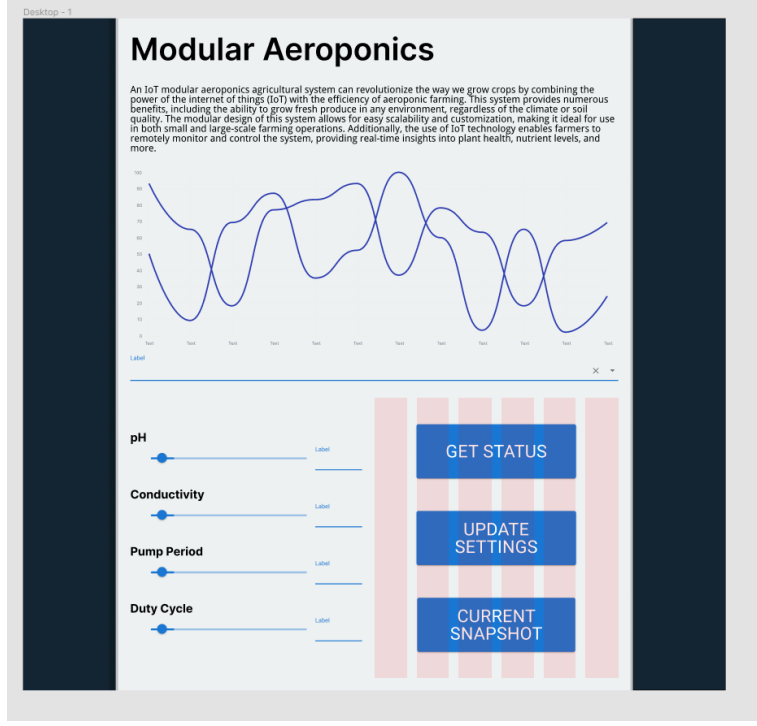


Figure 6.4: Control system user interface

Figure 6.4 above shows the completed design. Repeated units such as the labeled slider with numerical inputs were implemented as Figma components, which allows modification of multiple instances by making a single change to the master instance. The layout of the various components was configured to respond dynamically to changing screen width, allowing users with different devices to experience a convenient and intuitive interface.

The web application has three main features. These features were chosen to provide the most important information in a clear and intuitive way. The first of these is a time series chart that plots a chosen parameter over a three day period. Users can choose the parameter from a drop down menu that is preconfigured with the types of environmental data that the module is monitoring. This allows users to get a simple overview of how tightly the environmental conditions are bound in their module.

The second feature is the ability to remotely adjust the control parameters of the aeroponics module. The pH and conductivity setpoints, as well as the on and off timing of the main pump, can be intuitively set using a slider or by directly inputting a value into an adjacent field. These setpoints can then be sent to the module by pressing the 'update settings' button.

The final feature is the ability to send a real-time request to the module and view

the environmental parameters of the module at the current instant. Users press the ‘get status’ button to prompt a report from the module, and then ‘current snapshot’ to get a pop-out display as in Figure 6.5 below. If the user presses the ‘current snapshot’ button before the ‘get status’ button, they will get a display of the last report. This will be the last automatic report from the module, which sends updates every hour by default. This feature serves two purposes. Firstly, it provides peace of mind to the user. Being able to interact with the module in real time gives reassurance that the module is functioning properly. Secondly, it allows the user to investigate any trends they may see in the time-series data. For example, if one parameter appears to be trending to an undesirable value, they can query the module and see if the past readings were anomalous or indicative of a possible fault in the system. This allows the user to limit their visits to the physical module to only those times when they are sure that the module needs to be assessed.

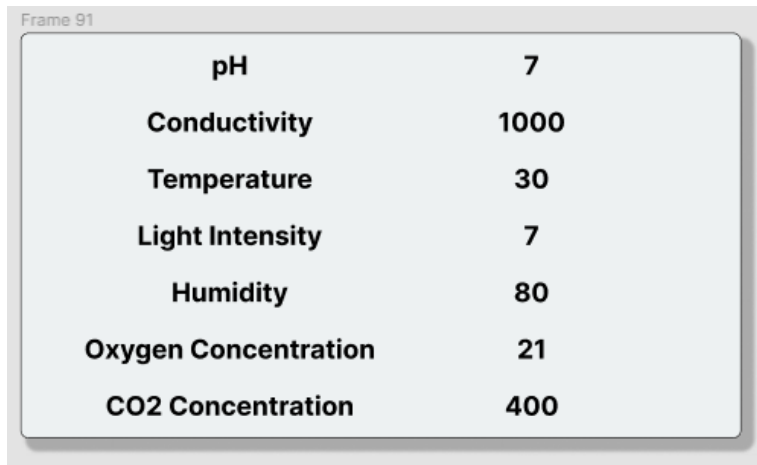


Figure 6.5: System parameters reading in user interface

Front end implementation: The front end was implemented using React. The Figma plug-in Locofy was used to convert the Figma design to React code. This process involved tagging the Figma design with HTML tags such as `<div>`, `<button>` and `<p>`. Locofy then outputs a configured React app with css stylesheets corresponding to the Figma design. Using the IDE Visual Studio Code, we then added functionality to the web application by adding API calls to the back end and linking the displayed data to the stored application data. We also added an authentication procedure, so that users have to register and log in to the application in order to view data and send commands. This prevents malicious attacks and adjustments by untrained and unqualified users.

Back end: To implement the back end we used Amazon Web Services. This was a practical choice for our project for two reasons. The first is that it provides a rapid solution across a range of different technologies that would otherwise require multiple experienced software developers. The second is that the solution is easily scalable. With no extra work and little cost, the solution can be expanded to any number of extra users.

To communicate with the aeroponics module, we used AWS IoT Core. This service allows secure MQTT communication between the AWS server and the ESP32 wifi

chip in the aeroponics module. MQTT (Message Queuing Telemetry Transport) is a lightweight communication protocol in which devices publish (send messages) and subscribe (listen to messages) on topics (channels). AWS provides a test suite in which developers can publish and subscribe to topics, which proved useful as a debugging and verification tool when implementing the web application and IoT setup on Arduino. AWS IoT Core also offers message routing to other AWS services, including databases (discussed more below). Our messages are structured according to JSON syntax, which allows them to be easily parsed and stored correctly for downstream tasks.

The database we use to store incoming data is AWS Timestream. Timestream automatically appends a timestamp to incoming data, which is useful for analyzing and visualizing trends over time. As the MQTT messages arrive to IoT Core, they are parsed and the information is sent to Timestream. Each data point is stored as a row in the database with the device name, parameter name, parameter value and timestamp as dimensions. Timestream can be queried remotely via the API using SQL, which is useful when initializing the web application.

To authenticate users, we use AWS Cognito. This service allows us to assign specific access rights to our AWS resources to authenticated users. Using AWS Cognito allows us to follow security best practices, which is beneficial to users as it ensures that their data is safe and that the messages coming to and from their aeroponics module cannot be intercepted. It is also beneficial to us, as it significantly reduces the likelihood of malicious attacks against our application. These attacks could sabotage our data and drive up usage based costs.

In order to integrate our AWS services with our React application, we used AWS Amplify developer libraries and the AWS software development kit (SDK) for JavaScript. Amplify libraries provide high-level APIs for a few of the most used AWS services including IoT Core and Cognito Authentication. Using Amplify significantly lowered our development time and allowed us to easily add dynamic, bidirectional functionality to the web application. To implement integration with AWS Timestream, we had to use the AWS SDK, which provides a lower level API compared to Amplify. However, the integration process was still smooth and authenticated users can now access their aeroponics module's stored time series data via the web application.

Arduino: The function of the Arduino in our system is to periodically read data from the various sensors connected to it, and then to generate and send reports of this data to a connected ESP32 chip. The Arduino is also responsible for sending signals to the relays that control power flow to the three pumps. We chose an Arduino Leonardo as it is cheap and has the necessary functionality.

The sensor signal types vary across the different sensors. The light, pH and conductivity meters output standard analog signals, the CO₂ meter outputs a PWM signal to a digital pin and the oxygen sensor communicates via I₂C. In order to obtain accurate values from the analog sensors, readings are taken every 40 milliseconds and stored in a buffer.

The CO₂ sensor data sheet provides sample code for reading the PWM signal from a digital pin on the Arduino. Similarly, the oxygen sensor has a custom library created by the manufacturer DFRobot that provides a simple API to read the oxygen concentration over I₂C.

To control the pumps, the Arduino simply sends a high or low voltage signal on each of three digital pins to the pump driver board. The control scheme for the main pump is basic, consisting of on and off periods calculated from user-provided values. These values are the pump period, which is the total period including pump on and off times, and the duty cycle, which is the percentage of the pump period for which the pump is on.

The control scheme for the pH and conductivity dosing pumps is more complex, taking into account the current value of the relevant readings and also the hysteresis of corrective action. A flow diagram of the control scheme is provided in Figure 6.6 below. As the figure shows, when the parameter value drops below the set point, the pump is switched on for a period of time. At the end of this period, it is turned off and the system enters a state of active waiting. During this period, the pump is not turned on even if the parameter value is below the set point. At the end of the active waiting period, the pump remains off until the parameter value drops below the setpoint at which point the control cycle will begin again.

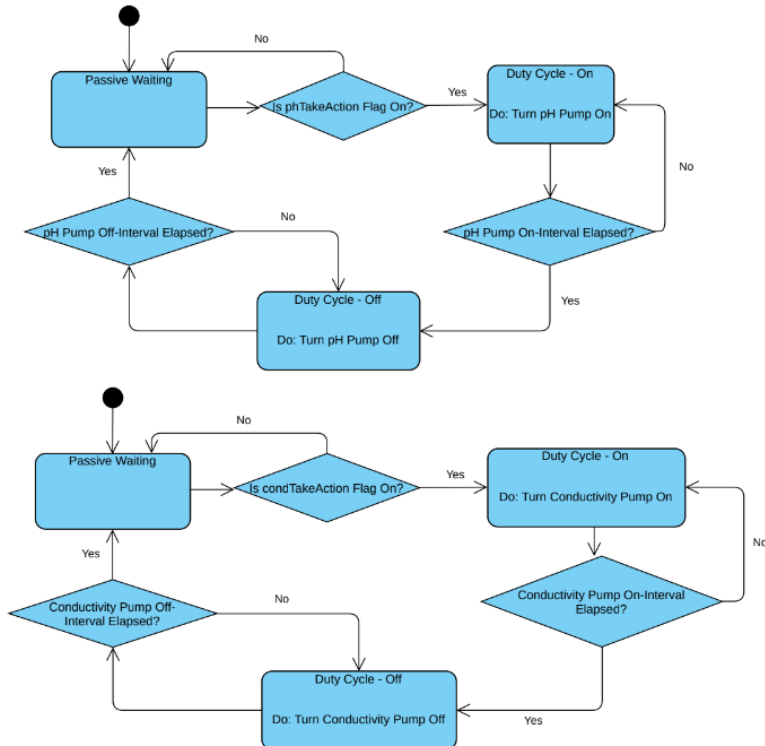


Figure 6.6: Control scheme for pH and conductivity adjustment

The Arduino receives requests from a connected ESP32 and responds to them according to the request. If the ESP32 sends an ‘update settings’ command, the

Arduino reads the subsequent values into its internal values and recalculates the on and off periods for the main pump. If the ESP32 sends a ‘send readings’ command, the Arduino generates a JSON message containing the parameter names and corresponding values and sends it via a serial connection to the ESP32.

ESP32: The role of the ESP32 in the system is to link the Arduino with AWS. It connects to the AWS servers over WiFi and establishes an MQTT connection. The ESP32 listens for requests from the web application and passes them to the Arduino over serial as described in the section above. It also automatically generates a ‘send data’ request periodically (every one hour by default). These automatically generated requests form the basis of the time series data recorded in the AWS Timestream database and visualized on the web application.

6.2 Issues Faced During Implementation

6.2.1 Structural Subsystem

The initial technical drawing shown in 6.1 did not have some necessary functionality details required by the growing module. Doors were required to access the interior of the system and wheels were needed to move it between different locations. Hence, they were added at the manufacturing stage. This proved useful both during the assembly of the module interior and for monitoring plant growth during usage. Attached to the bottom of the module were height-adjustable caster wheels. These make the module portable and allowed us to transport it from the machine shop to the desired spaces on campus.

Some of the challenges to the structural system and the envelope were that the doors to the module did not seal well, compromising the ability of the module to maintain a stable internal environment. Further, the cladding was not tightly secured to the aluminum framing resulting in sizable gaps between the walls and the framing away.

When transporting the module, the screw connecting one of the castor wheels to the frame buckled. This made further transportation very difficult and seriously undermines the portability of the module, which is one of its key design features.

6.2.2 Hydraulic Subsystem

During the implementation of the hydraulic subsystem, several issues were encountered that caused problems with the system’s performance. One of the most significant issues was the leakage that occurred around the nozzles and at the connection points between the different parts of the system. This leakage not only resulted in a loss of hydraulic fluid, but also affected the system’s ability to function properly. Another issue was that the duct tape kept falling off due to its exposure to water and to the humidity of the environment inside the model. Also, the setup of the drain does not allow easy access to the pipe with the nozzles, which will be needed for any nozzle repairs, changing the elevation of the horizontal pipe, and placing and harvesting plants.

Another potential issue that was encountered during the implementation of the hydraulic subsystem was the possibility of the mist from the nozzles not reaching the roots of the further plants. This was due to the fact that the roots of the closer plants could block the mist, resulting in uneven distribution of water and nutrients to the plants.

6.2.3 Thermodynamics

There was not enough insulating material in stock at NYU Abu Dhabi to cover all surfaces of the module. Therefore, we only put insulation on the top surface of the module. The effect of this change is that the module will be much more susceptible to heat flow via conduction, which will limit its ability to maintain its internal temperature below the identified threshold of 30°C in high ambient temperatures. Additionally, the power supplied to the module required an extension cord that was passed from outside the module to its interior. This caused the door to be slightly ajar. Ideally, the cord would pass through a grommet in order to create a thermal seal. However, this was not possible as the extension cord was borrowed and already had a plug attached to the end that we could not remove.

6.2.4 Electrical Subsystem

Our initial design did not include a switching mechanism for the three pumps. As a team we had experience using relays for controlling power supply to devices operating on low voltage DC power, but we had never done the same for appliances running off mains electricity.

We also faced multiple issues when calibrating the sensors. The first issue was a lack of adequate power to the sensor array. This issue was evident by the fact that the oxygen sensor would get stuck during initialisation and freeze the test program. Online research did not provide an obvious answer, and testing of the voltage input to the oxygen sensor breakout board revealed a supply voltage of only 4.6V. At this point, the power for all of the sensors was being supplied by the output pins of the Arduino.

A second issue was that the pH meter did not output reasonable values when the analog reading was converted using the code supplied in its datasheet. Upon testing we noticed that the output did differ by a few hundred millivolts when dipped in water compared to vinegar.

A third issue was that the assembled electrical system consisting of the pumps, microcontrollers, sensors and other boards was very messy and inconvenient to transport, repair and use. Sensor wires frequently became tangled with each other, limiting the distance that each sensor could be extended away from the Arduino. When changes needed to be made involving resoldering wires, the whole system including pumps had to be transported to the soldering station. This was inconvenient and unsafe, as the plastic insulation from other wires often obstructed the area that required soldering.

After transporting the module into the A5 atrium, the on-chip WiFi antenna was not powerful enough to connect to the NYU network. This made it difficult to debug the data collection system and necessitated a change to the hardware.

6.2.5 Software

Despite testing each sensor individually to verify that they could interface with the Arduino correctly and output accurate results, we faced issues when running the sensor system as a whole. The oxygen sensor took several seconds to transmit messages over I2C, whereas it should only take a few milliseconds. This led to errors transmitting information between the boards, as the receiving board would time out before the full sensor data had been submitted. Additionally, even when the Arduino was able to send a complete message to the ESP32 the data would often arrive corrupted and unreadable. We were able to identify the error as being caused by the carbon dioxide sensor, which was constantly sending interrupts that interfered with the interrupts used by the I2C and UART libraries.

6.3 Changes Made During Implementation

6.3.1 Structural Subsystem

To improve the seal around the doors, we ordered sealing tape to line the edges of the door frame with it. This would have allowed us to achieve a tight seal and aid in maintaining a regulated internal environment. However, it did not arrive in time to implement on the displayed model. To reinforce the broken castor wheels, we recommend the design of steel plates to transfer more of the lateral load that arises during movement to the frame. However, we did not have time to implement this design in time to fabricate it and add it to the displayed prototype. The completed manufactured system is shown in figure 6.7.

6.3.2 Hydraulic Subsystem

To ensure that the nutrient solution reaches all plants evenly, we addressed the issue of uneven distribution of mist from the nozzles by suspending the pipe using adjustable Velcro suspenders. In the initial design, there was a PVC pipe instead of the hose, and the hose allowed to adjust the elevation of the horizontal pipe before growing new species of plants. However, with the Velcro suspenders, the height of the pipe can be easily adjusted as needed during as the plants are growing to ensure that the mist reaches all plants, regardless of their distance from the nozzles. By adjusting the height of the pipe, we will be able to deliver the nutrient solution to the further plants as well as the close ones, ensuring that all plants received the appropriate amount of water and nutrients for optimal growth. Additionally, Velcro was used instead of duct tape for the drain, as it is waterproof, and the drain can easily be removed to allow access to the pipe and plants.



Figure 6.7: Photo of the completed manufactured growing system

6.3.3 Thermodynamics

The results in section 9.3.2 indicate that changes to the implementation are necessary for future iterations. In order to reduce heat flow from incident solar radiation, a shade cloth should be used to limit the sunlight reaching the module to that required for the growth of the plants. Alternatively, a material with very low absorptivity such as aluminium foil or an aluminium-based paint should be applied in a thin layer to the top surface.

Additionally, future implementations should include a grommet through which the external power cord can go without causing a leak. Sealing tape should also be used to create a thermal seal between incident faces and between the closed door and the module wall. These changes to the implementation will improve the module's ability to maintain the temperature and humidity of its internal environment within ranges suitable to plant health.

6.3.4 Planting Subsystem

At this stage of the design process, we identified that the railing system for the plant wells would be difficult to implement because it would require bespoke extruded railings and hence, it would not be easily accessible in developing markets that we are trying to access. It would also risk damaging the plants as the top of the basket would have to slide along the roof of the module. Further, it is important that plants can be removed individually without disturbing other plants. Situations where this would be useful include when one plant becomes sick and requires quarantine and treatment, or when one plant is ready to be harvested and others are not.

Given that the initially proposed railing system for installing of the plant baskets was not feasible, we decided on a system where the movement of the plant is not restricted until it is in place at which point it is securely fastened. We decided to attach the plants to the ceiling of the growing module using Velcro which is easily

accessible on the market. To hold the plant wells, we propose our unique design that will be 3D-printed. The design is shown in figure 6.8. In rural conditions, these baskets can be manufactured by gluing Velcro strips to the roof of the module and attaching parallel wooden strips to the rim of each basket. The plant could then be raised up through the hole in the roof from below, with the wooden strips orthogonal to the Velcro on the roof. A second strip of Velcro can then be placed on top so that the wooden strips are suspended between the two layers of Velcro.



Figure 6.8: 3D render of the plant bucket design

6.3.5 Electrical Subsystem

To control the power supply to the pumps, we met with Amjad Hamad of the Engineering Design Studio in the ERB. The design brief was to be able to control the switching of the three pumps via signals from the Arduino. Amjad designed a circuit that fed the signals from the Arduino to mechanical relays that controlled the power supply to the three pumps. Mains power was fed to the board by connecting the output of the 230V/120V AC/AC transformer to the board. This was achieved by cutting off the plug on one end of a cable and crimping FASTON receptacles to the line and neutral wires. These were attached to corresponding FASTON flat tabs on the pump driver board. The pumps were attached to the board in similar fashion. On the pump driver board, the neutral tabs were shorted and power supply was limited by separating the input line voltage from the line tabs with relays.

A reliable 5V DC power supply for the microcontrollers and sensors was achieved by soldering a 120-230V AC/5V DC transformer to the pump driver board and the sensor array power rails. This transformer provides sufficient current to the sensors and has ample input power as it is connected to mains power.

The pH sensor was calibrated manually, by reading the analog output when the sensor was immersed in solutions at 4, 7 and 10 pH. A line was then fit through the three points and used to derive an equation relating pH to the analog output of the

sensor.

To organize the electrical system, we placed the control boards and microcontrollers in a plastic lunchbox and punched holes in the side to pass wires through. This prevents the wires from getting tangled as the holes are separated from each other. Also, with the FASTON connections mentioned above for the pumps and mains power supply, the largest components can be easily disconnected and reconnected. The sensors are attached to the Arduino via breadboard jumper wires, so they can also be disconnected and reconnected relatively easily. These adjustments make the system much neater, more portable and more easily repairable compared to the original design. Importantly, it is also much safer as the high voltage terminals to which the pumps are connected are no longer exposed but rather stowed at the bottom of the tank.

The range of the WiFi receiver was increased by soldering an antenna to the ESP32 microchip. This required scraping off the solder mask covering the on-chip antenna and severing the existing connection to it. The shield and center of the coaxial cable comprising the antenna were then soldered to the corresponding traces on the ESP32 development board. This change increased the Received Signal Strength Indicator (RSSI) of the NYU network from 82 to 45dB when testing indoors, and allowed the chip to detect the network with an RSSI of 83dB inside the atrium.

6.3.6 Software

To fix the communication issue between the Arduino and ESP32, we removed the carbon dioxide sensor that communicated via an interrupt-driven codebase and replaced it with one that output a simple analog signal. This change allowed the I2C communication between the Arduino and the oxygen sensor to occur uninterrupted and reduced the time taken to read the sensor from around 10 seconds to a few milliseconds. The ESP32 was also able to receive intact messages occasionally, however they were sometimes still corrupted. To fix this, we reduced the baud rate from 115200 bit/s (which we use for the debug serial communication with the computer) to 9600 bit/s. This reduces the likelihood of information loss due to the surrounding electrical noise, and does not impact performance as there are no high-speed components in the system.

6.4 Initial Results

6.4.1 Structural Subsystem

The performance of the structural system was observed during operations of the unit. As discussed in subsection 4.2.1, the structural system was expected to easily sustain any loads applied by the growing system. For reference, the vertical shear force fill diagram for the frame is shown in figure 6.9 and the bending moment fill diagram is shown in figure 6.10. The maximum values of vertical shear force and bending moment are experienced by the long bottom members.

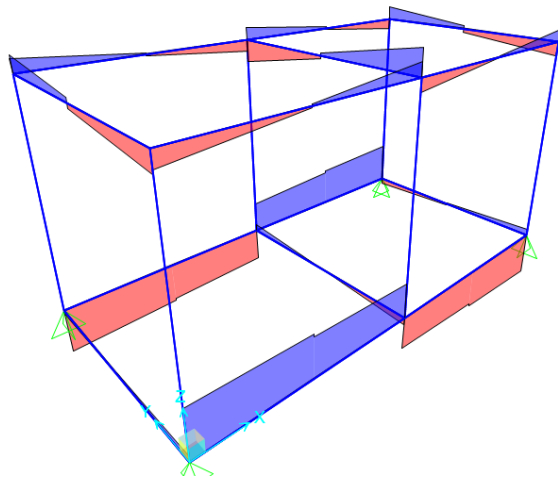


Figure 6.9: Vertical shear force fill diagram for the frame

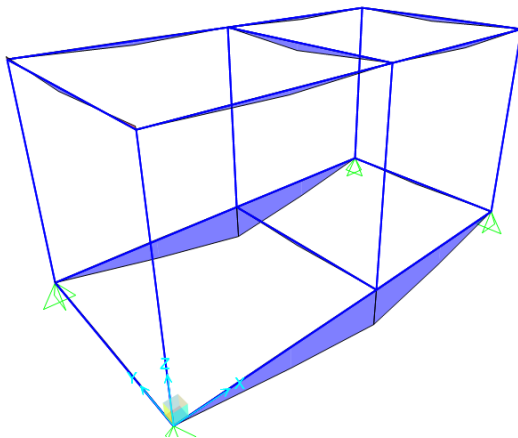


Figure 6.10: Bending moment fill diagram for the frame

6.4.2 Hydraulic Subsystem

It was hypothesized that the water could reach a distance of 0.44 m from the nozzles, which meant that plants placed up to that distance away from the pipe would receive the nutrient solution.

To test that hypothesis, a plastic sheet was placed under the pipe with markings at different distances (0.15 m, 0.30 m, and 0.44 m) to check if the nutrient solution misted from the nozzles reach those distances. The reason for choosing those distances is that we have plants 0.15 m and 0.30 m away from the pipe, and 0.45 m is the distance that was hypothesized as the maximum distance that the nutrient solution could reach from the nozzles.

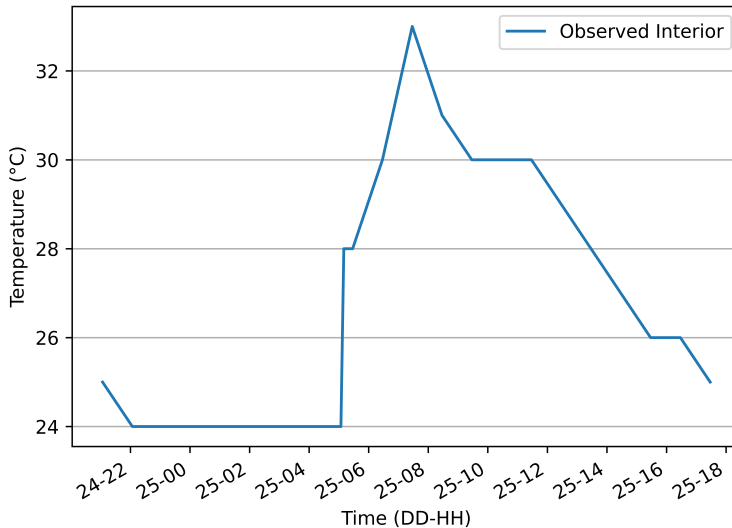
We have observed that some nozzles were faulty. Specifically, the nozzle that didn't mist the solution to a distance of 0.15 m from the pipe misted the solution at a downward trajectory. We also observed discontinuous water flow from some of the nozzles.

Table 6.1: Results for distance the solution travels from the nozzles

Distance from pipe (m)	Number of successful nozzles
0.15	23 out of 24 nozzles
0.30	13 out of 24 nozzles
0.44	0 out of 24 nozzles

6.4.3 Thermodynamics

The initial results of the system are shown in Figure 6.11 below. These results indicate that the system is able to read data inside the module correctly and that the module is largely able to keep the temperature in the system below the upper limit of 30°C. One feature of note is the sharp temperature increase at 0530-0800, followed by a steady decline over the rest of the day. Explanations for this temperature pattern and their effect on our design are discussed in section 9.3.



6.4.6 Software

The database was populated with data from the aeroponics module, indicating that the software connecting the Arduino to AWS was working properly. The web application also displayed data correctly and allowed us to change the module's settings remotely.

Chapter 7

Ethics

The ethical concerns for this project are not significant. An issue to be considered is the carbon footprint of the system. With climate change on the rise, sustainability should be a priority for all engineers. Although aeroponics is a sustainable alternative to traditional farming as plants require less nutrients and water, the added equipment that help maintain the optimal conditions for plant growth like artificial lighting and fans can increase the system's carbon footprint, unlike traditional farming where plants are exposed to sunlight and natural wind. This is an issue to be considered, however, by building a system that is not fully-controlled, we will be able to limit the carbon dioxide emissions.

A potential ethical consideration is the decision about using genetically modified seeds in the growing system. However, this is an issue pertaining to the field of agriculture rather than engineering and it is beyond the scope of this project. Hence, it is not further discussed.

Chapter 8

Impact of Covid-19

The Covid-19 pandemic had limited effect on our project. However, it did impose constraints on our planning and preparation during the early stages of the project. Due to changes in the engineering program structure resulting from the pandemic, all of our group members were at the New York campus for both the Fall and Spring semesters of our Junior year. This meant that we were not able to physically meet our advisors or industry contacts while we were in the process of conceptualising the project and writing the initial proposal.

Another impact of Covid-19 on our project was its effect on global supply chains. Many of the parts required for our project were shipped from the United States, and this process took more than a month. However, imports into the UAE often take a long time to be cleared from border control so the slow shipping may not have been significantly impacted by Covid-19.

In general, Covid-19 did not have a significant impact on our project. This is particularly because the bulk of our work was conducted in the Fall semester of 2022 and the Spring semester of 2023, after the Covid-19 restrictions had largely been removed from campus.

Chapter 9

Evaluation of Design

9.1 Criteria for Testing

The goal for the project was to suggest an optimal design of a low-cost aeroponics system by looking into flows and losses of heat, gasses, water and nutrients. Testing of the system focused on analyzing the use of different structural materials, monitoring selected parameters in the system for the purpose of testing the design and detecting and responding to faults in the system. The gathered data was used to evaluate the design of the structure and the responsiveness of the monitoring system. The data was compared to known optimal conditions for aeroponics facilities. The initial plan was to compare in real-time the conditions achieved in our system with conditions obtained in a full-scale aeroponic system managed by Madar Farms in Kizad in Abu Dhabi. Madar Farms facilities use high-tech aeroponics systems that would serve as a benchmark for optimizing our design to get its performance as close as possible to the performance of high-tech systems with controlled environments. However, due to bankruptcy of Madar Farms, this collaboration was not implemented.

To satisfy the purpose of our project, our design must meet certain criteria that were outlined in section 1.4. For reference, these constraints are summarized in table 9.1. These constraints correspond to constraints anticipated when implementing the system in developing countries. Our design was evaluated on the strength of the structure, thermal stability of the growing unit (should be less than $0.3 \text{ W}/(\text{m K})$), its resilience to power outages (around 5 hours daily), water consumption, nutrient usage, responsiveness of monitoring system, technical knowledge needed to operate the system and total cost of design.

9.2 Test Data

9.2.1 Size, Weight and Structural Integrity

The size of the manufactured module is 1 m long, 2 m wide and 1 m high. The weight of the timber module with hydraulic system filled with water would be 14 kg. The weight of the manufactured aluminium frame module with hydraulic system is 25 kg.

The maximum values of forces and stresses for the manufactured module are shown

Table 9.1: Criteria for design evaluation

Criteria	Quantification
Technical	
Size	Max. 1 m x 2 m x 1 m
Weight	Max. 20 kg
Structural integrity	$\tau_{max} < \tau_{all}$, FS = 1.2 $\sigma_{b,max} < \sigma_{b,all}$, FS = 1.2 $d_{max} < 0.03$ m, FS = 1.2
Internal environment control	$T_{max} < 30^\circ C$ Humidity $\leq 85\%$
Power demand	$P_{max} < 1$ kW
Water consumption	< 1% water loss
Internet connectivity	< 1 Mbps (3G)
Non-technical	
Modularity and portability	
Total cost	< 1000 USD
Technical knowledge	
Growing capacity	50kg/month

in table 9.2, given T-slot beams and columns with 4 cm x 4 cm cross-section. The results were computed in SAP2000. The distribution of stresses was not measured experimentally. Only the maximum deflection of the center of the beams from the end was measured experimentally. No deflection was observed.

Table 9.2: Internal forces and moments for aluminium frame

Dimension	V_{max} [N]	τ_{max} [MPa]	M_{max} [Nm]	σ_{max} [MPa]	d_{max} [m]
4 x 4	221.06	0.32	190.17	-26.09	0.007

9.2.2 Internal Environment Control

The temperature and humidity inside the module were measured over three days. These measurements took place while the module was switched off, to simulate its resilience to power outages. The results are shown in the figures below and discussed extensively in section 9.3.2.

9.2.3 Water Consumption

The system's water consumption was tested. For 12.5 liters of water placed in the tank at the beginning of the 5-day growing period that we had, around 60 ml of water was consumed by the system. During that period, we had 12 plants, which is the half capacity of our model. Assuming that having full capacity will double the water consumption, then the system will still consume less than 1% of the water.

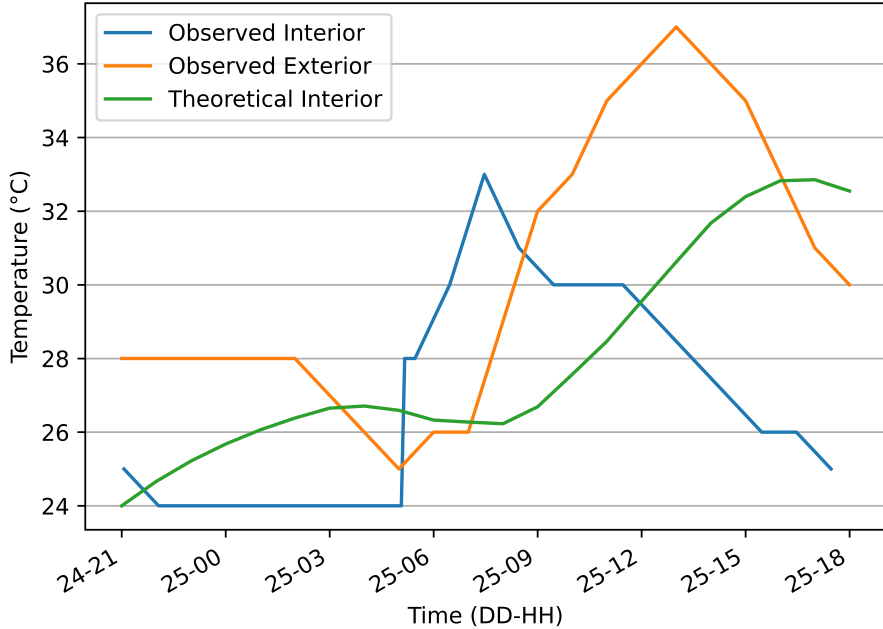


Figure 9.1: Observed temperatures inside and outside the module over one day. The theoretical temperature inside the module considers conduction only.

9.2.4 Power Demand and Internet Connectivity

The power usage of the aeroponics module was assessed by measuring the current through the AC and DC subsystems and multiplying them by the respective voltage levels of the two systems (110V and 5V, respectively). The AC current was measured using a clamp meter, which enabled us to measure the current without breaking the circuit. The DC current was measured using a ammeter connected in series with the output of the AC-DC transformer. Both sensors were interfaced with a data acquisition system to record the current as a timeseries.

Figure 9.4 shows the observed power usage and current consumption while the aeroponics module was operating with a ten minute period and ten percent duty cycle. The green and blue traces represent the AC and DC current, respectively. The plot shows that the DC current fluctuates between 0.5A and 0.6A as calculated in section 3.1.5. The occasional large spikes can be explained by the extra current drawn by the ESP32 when sending a message. The AC current fluctuates around 0.02A when the main pump is off and 0.3A when the main pump is on. This is again in line with the data provided by the manufacturer. During this observation period, the dosing pumps did not turn on so their contribution to the AC current consumption is not measured here.

The red and orange traces show the power usage of the AC and DC subsystems. These signals follow the corresponding current signals according to Ohm's power law ($P = IV$). The total power lies around 4W when the pump is off and 36W when it is on. These values are slightly higher than those calculated in section 3.1.5. We assume that this is due to inaccuracies in the data obtained from the datasheets provided by the manufacturers of the pumps and sensors, and also to inefficiencies in the AC-DC transformer and voltage regulators on the sensor breakout boards

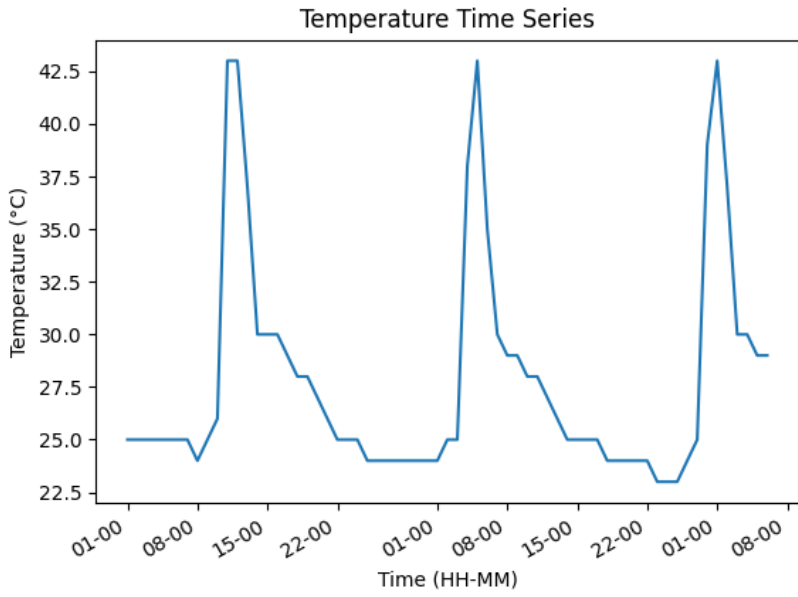


Figure 9.2: Observed temperature inside the module

that were not initially accounted for. However, 36W is still well under the identified constraint of 1kW.

The bandwidth usage of the aeroponics module was monitored by downloading the opensource network analysis software Wireshark and using it to track the packets sent by the ESP32. Figure 9.5 shows the bandwidth usage of the ESP32 over ten minutes while it was sending message every minute. The package sizes were around 150 bytes and took around one second to send, so the bandwidth usage was around fluctuated around 150 bytes/s during message transmission. Message reception was not measured here, but would be in the same region. This value is much lower than the identified constraint of 3Mbps. It is even much lower than the bandwidth offered by 2G networks (0.1Mbps), so our module is able to remain online in areas that rely on 2G networks.

9.2.5 Non-Technical Constraints

As shown in the budget in table 5.1, the total cost of the suggested design is 911.33 USD. The final cost of manufacturing of the prototype is 2610.70 USD, as shown in table 5.2.

In terms of portability, the design would be equipped with wheels that enable portability and hydraulic components that enable connecting several modules into one setup.

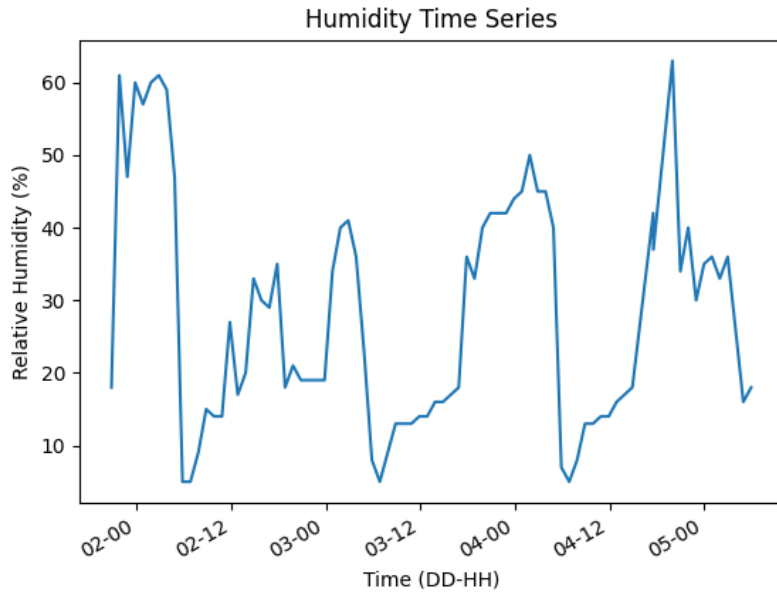


Figure 9.3: Observed humidity inside the module

9.3 Discussion

9.3.1 Size, Weight and Structural Integrity

The size of the implemented module meets the design criteria. The weight of the manufactured prototype exceeds the design criteria of 20 kg. This is because the prototype was build with aluminium frame which has density greater than timber which was initially proposed as structural material. If the frame was made out of timber, the design constraint would be met.

Given shear strength of aluminium of 207 MPa and bending strength of 300 MPa, the computed stresses are well below the maximum allowable stresses. The frame is not expected to deform or break. Indeed, the structural components did not fail and no deflection was observed. The system maintained its structural integrity. We anticipate if the module would be manufactured according to the initial design, with timber, it would also not exhibit any deflection or bending.

While the basic design criteria were met, further research in this area could focus on finding the optimal materials and shape of structural components that would carry the load while minimizing the cost, size and weight of the system. Many composite materials, such as fiberglass, would be available to minimize the weight, however, it is not obvious what materials could replace timber in low-cost applications.

9.3.2 Internal Environment Control

The temperature of the inside of the module is shown in Figure 9.1, along with the external ambient temperature and the predicted internal temperature based on pure conduction.

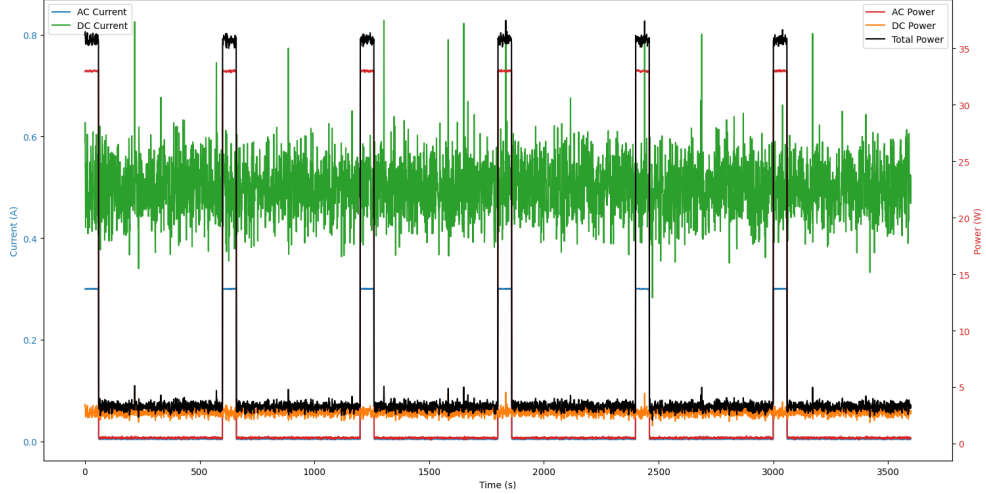


Figure 9.4: Power usage and current flow through the AC and DC subsystems of the aeroponics module over a one hour period

The theoretical model uses the combined thermal resistivity from section 3.1 for the case with polyurethane foam insulation to calculate the heat flux through one square meter of the module. The temperature at the outer surface is taken as the current observed external temperature and the temperature at the inner surface is taken as the temperature inside the module at the current step. The heat flux is then multiplied by the surface area of the module and the temperature rise is calculated by assuming that all of the heat flow goes into heating the water/air mixture inside the module. The model assumes that the total mass of water in the module, including in liquid form in the tank and as vapour in the air, is 10kg. The combined specific heat capacity of the water and air inside the module is shown below.

$$\begin{aligned}
 (mc)_{total} &= m_{air} \cdot c_{air} + m_{water} \cdot c_{water} = \rho_{air} \cdot V_{air} \cdot c_{air} + m_{water} \cdot c_{water} \\
 &= 1.293 \text{ kg/m}^3 \cdot 2 \text{ m}^3 \cdot 1.005 \text{ kJ/K} + 10 \text{ kg} \cdot 4.18 \text{ kJ/kg} = 44.4 \text{ kJ/K}
 \end{aligned}$$

The formula used to iteratively calculate the theoretical temperature inside the module is given below.

$$T_{t+1} = \frac{\dot{Q} \cdot \Delta t}{(mc)_{total}} + T_t$$

It is clear from Figure 9.1 that the observed temperature inside the module does not closely follow the theoretical model. The most intriguing feature of the plot is that while the theoretical temperature lags the external temperature, as we would intuitively expect, the observed temperature actually peaks before the external temperature. This behaviour was repeated very closely over three days as shown in Figure 9.2.

The unexpected temperature rise can be explained by the positioning of the module during this testing period. The module was kept at the southern edge of the A5 atrium, which meant that it was in the shade for the whole day excluding the early morning. As the plot shows, the temperature peaked sharply during the

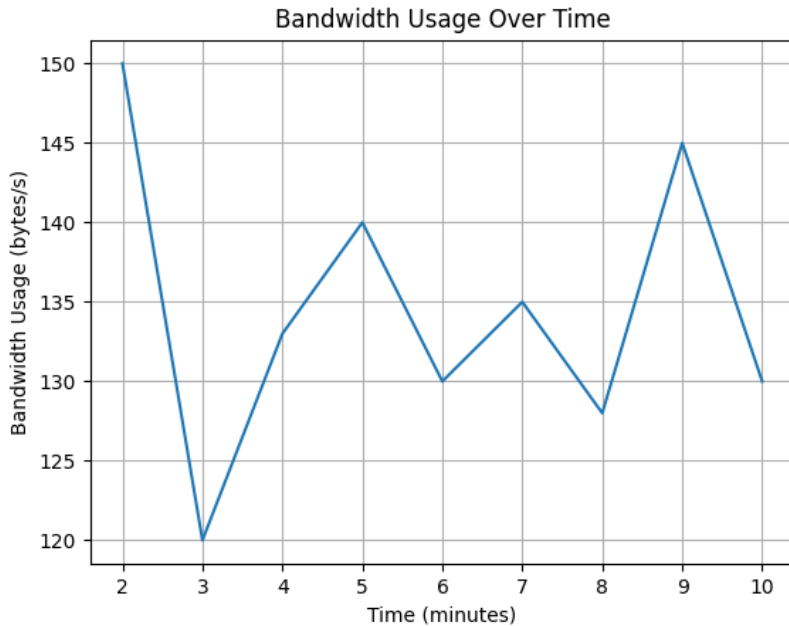


Figure 9.5: Bandwidth usage by the aeroponics module over ten minutes

exact period that it was exposed to sunlight (0600 and 0800). This resulted in the module consistently heating to around 42°C, around 15°C warmer than the ambient temperature at the same time. Figure 9.6 shows that the predicted time taken for the module to heat up from 20°C to 25°C is around three minutes. The heat flux used in this simulation is calculated by assuming that the solar radiation reaching earth's atmosphere (1300W) diminishes to 400W by the time it reaches the surface. Although the heat flow through the insulation will not be fully 400W as modelled below, the high absorptivity of the black coating on the plywood cladding and polyurethane foam will result in the outer surfaces of the module reaching much higher temperatures than surroundings and increasing the rate of conduction through the insulation significantly.

Our initial design featuring retrofitted polystyrene insulation would have alleviated this problem to some extent, as the absorptivity of polystyrene is lower than that of black paint (approximately 0.5 compared to 0.95). However, this value still results in heat flow due to solar radiation that dominates that due to ambient conduction. Based on the results of section 3.2.3, the heat flow due to conduction through polyurethane foam at 40°C ambient temperature is 13 W/m² and 104 W for the whole module. By comparison, assuming $\alpha = 0.5$ for polystyrene the heat flow at the top surface is:

$$400W/m^2 \times 0.5 \times 2m^2 = 400W$$

In order to reduce this value significantly, a material with a very low absorptivity should be attached to the outer surface. Alternatively, a shade cloth should be used to cover the surface of the module during strong sunlight. One such material with low absorptivity is aluminium foil. Aluminium foil has an absorptivity around 0.05 [26], so it reflects 95 percent of incident thermal radiation. This would reduce the heat flow at the top surface by an order of magnitude as follows:

$$400W/m^2 \times 0.05 \times 2m^2 = 40W$$

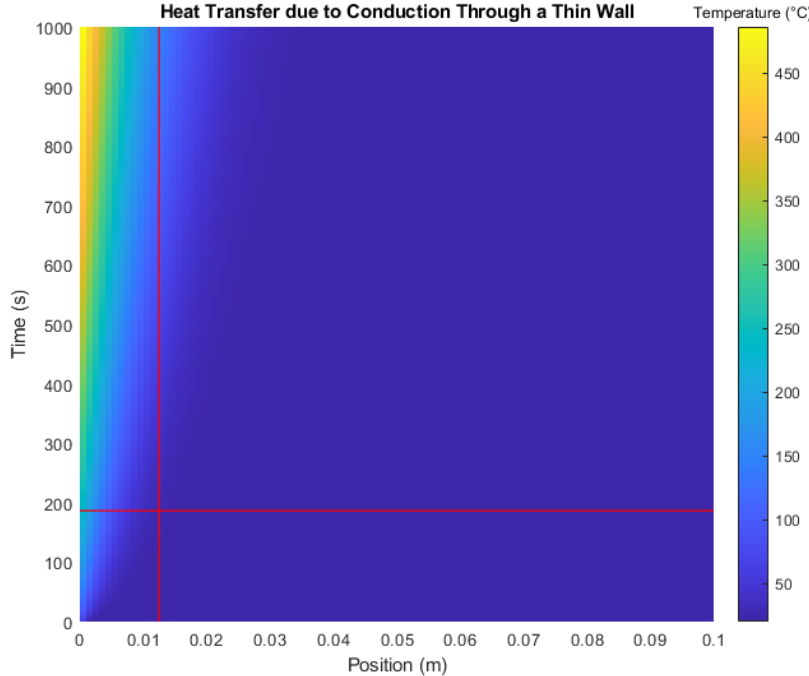


Figure 9.6: Simulated conduction through the module's upper surface with solar radiation heat flux boundary condition

One drawback to using aluminium is that the emissivity of aluminium can be less than its absorptivity for some surface finishes and alloy compositions [26]. This would result in the foil heating up significantly in sunlight, creating a fire hazard and a high rate of thermal conduction through the insulation beneath it. However, this can be avoided by ensuring that the chosen aluminium foil has an absorptivity less than or equal to its emissivity.

We conclude that when constructed according to our suggested design, our module has the necessary insulation to resist a detrimental increase in its interior due to conduction from the outside in realistic temperatures (up to 40°C). Outside of direct sunlight, its internal temperature did not increase beyond the identified maximum. Further, we offer a solution to significantly reduce the impact of solar radiation and therefore suggest that the module is capable of resisting internal temperature changes in adverse external conditions for long enough to alert the user to take corrective action. In the worst case scenario considered (40°C ambient temperature and strong sunlight), it will take almost half an hour for the module to heat up by five degrees as shown below:

$$\dot{Q}_{total} = \dot{Q}_{conduction} + \dot{Q}_{radiation} = 108W + 40W = 148W$$

$$\Delta t = \frac{\Delta T \times (mc)_{total}}{\dot{Q}_{total}} = \frac{5K \cdot 44400J/K}{148J/s} = 1500s$$

It is clear from Figure 9.3 that when the module is turned off, it does not regulate the internal humidity well. The humidity fluctuated in a regular pattern, peaking around 60 percent around 0300 and decreasing to almost zero around 0600 (corresponding to the peak in internal temperature discussed above). This pattern can be

explained by the humidity of the external environment, indicating that the interior of the module was not a closed system.

The results of section 3.2.3 indicate that in order to achieve cooling, water must evaporate from the nutrient tank. This will cause the relative humidity of the module to rise until it saturates. Therefore, we expect that by improving the sealing of the module through the implementation changes referred to in section 6.3.3 the relative humidity of its interior will remain above the threshold value of 85 percent.

9.3.3 Water Consumption

The water consumption of our aeroponics system proved to be remarkably efficient, amounting to less than 1% of the overall usage. This achievement aligns perfectly with the technical constraint we established, and it bears significant benefits. By consuming minimal amounts of water, our model demonstrates a commendable level of sustainability and resource conservation. This aspect is particularly advantageous in regions where water scarcity is a pressing concern. Moreover, the reduced water usage contributes to lower operational costs, making our aeroponics system not only environmentally friendly but also economically viable. The exceptional efficiency in water consumption achieved by our model showcases its ability to optimize resource allocation while maintaining optimal plant growth conditions, highlighting its potential for widespread adoption in future agricultural practices.

9.3.4 Power Demand and Internet Connectivity

The implemented software provides a sleek interface for the aeroponics module, allowing the user to easily view historical data, change key settings remotely and get live status reports from the module if it is connected. These are key features in allowing the user to effectively interact with the module without imposing a large burden of required knowledge.

However, there are other important features that we did not have time to implement. The first of these is a dropdown list of crops for the user to select. When the user selects a crop, the pH, conductivity and pump period setpoints would automatically adjust. Also, red horizontal lines would be added to each chart to indicate the upper and lower bounds of the acceptable range for each parameter. This would allow the user to easily see whether the module is maintaining its internal environment correctly for the specific crop that is being grown.

Another important feature that we did not have time to implement is automatic warning messages that are sent directly to the user. It would be beneficial if the user received messages via SMS and/or email if the module becomes offline or if any of the important environmental parameters such as temperature, pH or conductivity are out of range. This would give the user the most time to act when faults occur and give them peace of mind that the module is functioning correctly otherwise.

We also recommend the design of a custom circuit board. This would make the electronic system much more compact, and would also keep it neater. Most impor-

tantly, it decreases the technical knowledge required by the user as they can simply purchase a ready made item and plug it into their system. Finally, it reduces the cost of the module by allowing the user to purchase the components at a low cost and low quantity.

The final feature that we had planned to implement but were not able to due to the limitations of time was a machine learning algorithm to predict faults in the system based on changes in the environmental data. This feature was referenced in section 1.2.1 and would have proved a valuable tool in assisting users with limited technical knowledge to effectively use the aeroponics module. If allowed, we intend to continue to collect data over the summer so that we have a training dataset that we can use to train such a model and include it in future software releases.

9.3.5 Non-Technical Constraints

The cost of the prototype exceeds the desired budget for the system by a factor of 2. However, this is due to two main factors. Firstly, many spare electronic and hydraulic parts were ordered in preparation for constructing the system. This was in case any components were damaged in the construction process or if there were any last-minute changes to the design. This cost would be optimized in future purchases when the specific design is known. Secondly, aluminium was used as the material for structural components and it is a relatively expensive material. In the suggested design for deployment in developing countries, timber is proposed as the structural material. By implementing these two changes, the resulting budget is 911.33 USD which is in line with the design criteria.

In terms of portability, one of the wheels in the prototype failed. This suggests that stronger wheels need to be implemented in future iterations of the design. However, overall, the system performed well when moved between different locations. The modularity conventions were not implemented in the prototype and would need to be tested in future iterations.

The growing capacity of the module was not able to be evaluated in practice due to the limitations of time and the availability of seedlings. The constraint identified in section 1.4 refers to the weight of potatoes produced by the module, as that is the crop that we initially designed for. However, we were not able to obtain potato seedlings so were forced to use microgreens and mint instead. These plants produce much less material than potatoes, so it is not useful to assess the module's performance based on its output with these crops. As the module was designed according to the parameters outlined in [7], we assess that it is capable of achieving the same level of production and therefore meets the identified constraint on growing capacity.

The technical knowledge required to operate the system is difficult to quantify. Many of the desired features were implemented: an intuitive graphical user interface accessible over the internet on any device, an automated dosing control system and bidirectional remote communication with the module. However, there were some useful features identified in section 9.3.4 above that we did not have time to implement. Overall, we would need to perform a survey asking users from non-

technical backgrounds whether they found the module intuitive and easy to use. For the time being, we conclude that the module is sufficiently easy to use as all that is required by the user is a few clicks on a website. Additionally, the hardware designs, software and firmware are all open source and accessible. This gives everyone the freedom to replicate our module.

9.3.6 Summary

The table 9.3 summarizes to what extent the design criteria were met.

Table 9.3: Design criteria evaluation

Criteria	Quantification	Evaluation
Technical		
Size	Max. 1 m x 2 m x 1 m	Met
Weight	Max. 20 kg	Not met for prototype, met for suggested design
Structural integrity	$\tau_{max} < \tau_{all}$, FS = 1.2 $\sigma_{b,max} < \sigma_{b,all}$, FS = 1.2 $d_{max} < 0.03$ m, FS = 1.2	Met for prototype and design Met for prototype and design Met for prototype and design
Internal environment control	$T_{max} < 30^\circ C$ Humidity $\leq 85\%$	Partially met for prototype, recommendations offered Not met for prototype, recommendations offered
Power demand	$P_{max} < 1$ kW	Met for prototype and design
Water consumption	< 1% water loss	Met for prototype and design
Internet connectivity	< 1 Mbps (3G)	Met for prototype and design
Non-technical		
Modularity and portability		Partially met for prototype, met for design
Total cost	< 1000 USD	Met for prototype and design
Technical Knowledge		Met for prototype and design
Growing capacity	50kg/month	Partially met for prototype, met for design

Bibliography

- [1] I. A. Lakhia, G. Jianmin, T. N. Syed, F. A. Chandio, N. A. Buttar, and W. A. Qureshi, “Monitoring and control systems in agriculture using intelligent sensor techniques: A review of the aeroponic system,” *Journal of Sensors*, vol. 2018, pp. 1–18, 2018.
- [2] D. Tilman, C. Balzer, J. Hill, and B. L. Befort, “Global food demand and the sustainable intensification of agriculture,” *Proceedings of the national academy of sciences*, vol. 108, no. 50, pp. 20 260–20 264, 2011.
- [3] I. A. Lakhia, J. Gao, T. N. Syed, *et al.*, “Overview of the aeroponic agriculture—an emerging technology for global food security,” *International Journal of Agricultural and Biological Engineering*, vol. 13, no. 1, pp. 1–10, 2020.
- [4] N. Sharma, S. Acharya, K. Kumar, N. Singh, and O. P. Chaurasia, “Hydroponics as an advanced technique for vegetable production: An overview,” *Journal of Soil and Water Conservation*, vol. 17, no. 4, pp. 364–371, 2018.
- [5] S. Ragaveena, A. Shirly Edward, and U. Surendran, “Smart controlled environment agriculture methods: A holistic review,” *Reviews in Environmental Science and Bio/Technology*, vol. 20, no. 4, pp. 887–913, 2021.
- [6] R. v. K. Jess Halliday and K. V. Herath, “An assessment of controlled environment agriculture (cea) in low- and lower-middle income countries in asia and africa, and its potential contribution to sustainable development,” Commission on Sustainable Agriculture Intensification, Tech. Rep., Nov. 2021.
- [7] V. Otazu, *Manual on quality seed potato production using aerponics*. International Potato Center, 2010.
- [8] I. Gnip, S. Véjelis, and S. Vaitkus, “Thermal conductivity of expanded polystyrene (eps) at 10 c and its conversion to temperatures within interval from 0 to 50 c,” *Energy and Buildings*, vol. 52, pp. 107–111, 2012.
- [9] M. H. Tunio, J. Gao, S. A. Shaikh, *et al.*, “Potato production in aerponics: An emerging food growing system in sustainable agriculture for food security,” *Chilean journal of agricultural research*, vol. 80, no. 1, pp. 118–132, 2020.
- [10] I. Idris and M. I. Sani, “Monitoring and control of aeroponic growing system for potato production,” in *2012 IEEE Conference on Control, Systems & Industrial Informatics*, IEEE, 2012, pp. 120–125.
- [11] M. E. Çalışkan, C. Yavuz, A. K. Yağız, U. Demirel, and S. Çalışkan, “Comparison of aerponics and conventional potato mini tuber production systems at different plant densities,” *Potato Research*, vol. 64, pp. 41–53, 2021.

- [12] A. AlShrouf *et al.*, “Hydroponics, aeroponic and aquaponic as compared with conventional farming,” *Am. Sci. Res. J. Eng. Technol. Sci*, vol. 27, no. 1, pp. 247–255, 2017.
- [13] farm.ws, *Aeroponics — definition, types, system, advantages cost*, Available at <https://farm.ws/aeroponics/>, Jun. 2022.
- [14] T. W. Gurley, *Aeroponics: Growing Vertical*. CRC Press, 2020.
- [15] I. Nir, “Growing plants in aeroponics growth system,” in *Symposium on Substrates in Horticulture other than Soils In Situ 126*, 1981, pp. 435–448.
- [16] I. Farran and A. M. Mingo-Castel, “Potato minituber production using aeroponics: Effect of plant density and harvesting intervals,” *American Journal of Potato Research*, vol. 83, pp. 47–53, 2006.
- [17] L. A. Peterson and A. R. Krueger, “An intermittent aeroponics system,” *Crop science*, vol. 28, no. 4, pp. 712–713, 1988.
- [18] I. A. Lakhia, J. Gao, T. N. Syed, F. A. Chandio, and N. A. Buttar, “Modern plant cultivation technologies in agriculture under controlled environment: A review on aeroponics,” *Journal of plant interactions*, vol. 13, no. 1, pp. 338–352, 2018.
- [19] C. Martinez-Nolasco, J. A. Padilla-Medina, J. J. M. Nolasco, R. G. Guevara-Gonzalez, A. I. Barranco-Gutiérrez, and J. J. Diaz-Carmona, “Non-invasive monitoring of the thermal and morphometric characteristics of lettuce grown in an aeroponic system through multispectral image system,” *Applied Sciences*, vol. 12, no. 13, p. 6540, 2022.
- [20] D.-H. Park and J.-W. Park, “Wireless sensor network-based greenhouse environment monitoring and automatic control system for dew condensation prevention,” *Sensors*, vol. 11, no. 4, pp. 3640–3651, 2011.
- [21] M. Pala, L. Mizenko, M. Mach, and T. Reed, “Aeroponic greenhouse as an autonomous system using intelligent space for agriculture robotics,” *Advances in Intelligent Systems and Computing*, vol. 274, p. 83, 2014.
- [22] K. Ferentinos, L. Albright, and B. Selman, “Neural network-based detection of mechanical, sensor and biological faults in deep-trough hydroponics,” *Computers and Electronics in Agriculture*, vol. 40, no. 1-3, pp. 65–85, 2003.
- [23] L. B. Tik, C. T. Khuan, and S. Palaniappan, “Monitoring of an aeroponic greenhouse with a sensor network,” *International Journal of Computer Science and Network Security*, vol. 40, no. 3, pp. 240–246, 2009.
- [24] O. Almanza, M. Rodriguez-Pérez, and J. De Saja, “Measurement of the thermal diffusivity and specific heat capacity of polyethylene foams using the transient plane source technique,” *Polymer international*, vol. 53, no. 12, pp. 2038–2044, 2004.
- [25] desertcart.ae, *Teku 500 2 inch net slit pots for hydroponic aeroponic use*, Available at <https://www.desertcart.ae/products/9529016-teku-500-2-inch-net-slit-pots-for-hydroponic-aeroponic-use>.
- [26] J. Frolic, T. Králik, V. Musilová, P. Hanzelka, A. Srnka, and J. Jelinek, “A database of metallic materials emissivities and absorptivities for cryogenics,” *Cryogenics*, vol. 97, pp. 85–99, 2019.

Project Management

Work Breakdown Structure (WBS)

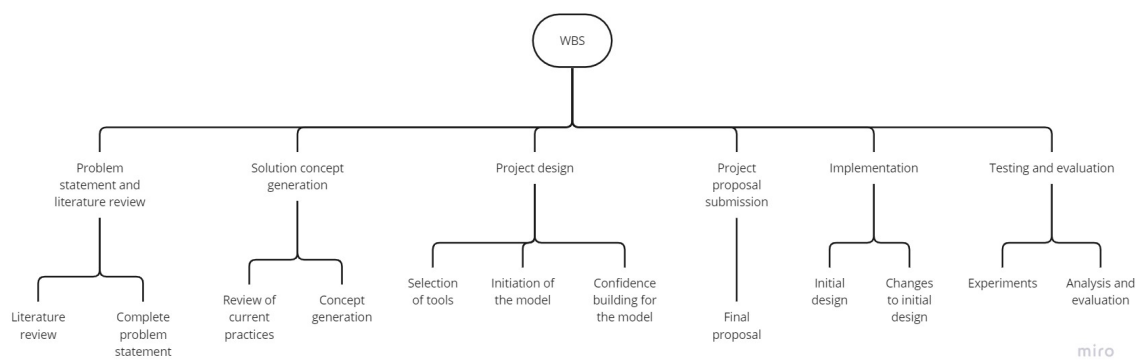


Figure 9.7: Work breakdown structure (WBS)

Dependency Structure Matrix (DSM)

Task	Subtask	Dependency	1	2	3	4	5	6	7	8	9	10	11	12
Problem statement and literature review	Literature review	1	0	0	0	0	0	0	0	0	0	0	0	0
	Complete problem statement	2	1	0	0	0	0	0	0	0	0	0	0	0
Solution concept generation and selection	Review of current practices	3	0	0	0	0	0	0	0	0	0	0	0	0
	Concept generation	4	1	1	1	0	0	0	0	0	0	0	0	0
Project design	Selection of tools	5	0	0	1	1	0	0	0	0	0	0	0	0
	Initiation of the models	6	0	0	1	1	0	0	0	0	0	0	0	0
	Confidence building for the model	7	0	0	0	0	0	1	0	0	0	0	0	0
Project proposal submission	Submission of the final proposal	8	1	1	0	1	0	0	1	0	0	0	0	0
Implementation	Initial design	9	0	0	0	0	1	1	1	0	0	0	0	0
	Changes to initial design	10	0	0	0	0	0	0	0	0	1	0	0	0
Testing and evaluation	Experiments	11	0	0	0	0	0	0	0	0	1	1	0	0
	Analysis and evaluation	12	0	0	0	0	0	0	0	0	0	0	1	0

Figure 9.8: Dependency structure matrix (DSM)

Gantt Chart and Critical Path

See Figure 9.9 below.

Changes Made to Project Management

The work process for our capstone was generally aligned with the WBS, the DSM and the Gantt chart outlined at the beginning of the process. However, based on the progress of the work, we had to update and re-align some of the tasks. Firstly, selection of the tools, ordering and delivery of the materials for the system took longer than expected, due to long lead times. Hence, we were not able to initiate the models until late November.

In the spring, the implementation, testing and evaluation stages had to be further broken down into specific tasks that we did not list down while the project outline was created. These tasks included assembling the system, prototyping alternative designs, running the experiments, collecting the data, analysing the results and benchmarking the results against industry standards. In particular, assembling the system and prototyping alternative designs took much more time than expected because we had to synchronise functioning of the hydraulic and mechanical systems. Due to issues with assembling them and missing materials, we had to seek support from the Advanced Manufacturing Lab at NYU Abu Dhabi. Hence, we were not able to finalize the design and run experiments until late March, which significantly reduced our ability to analyze data from different experimental trials. Given these challenges and constraints, we had to continuously revise the anticipated timelines and ensure that our updated Gantt charts do not violate the critical path.

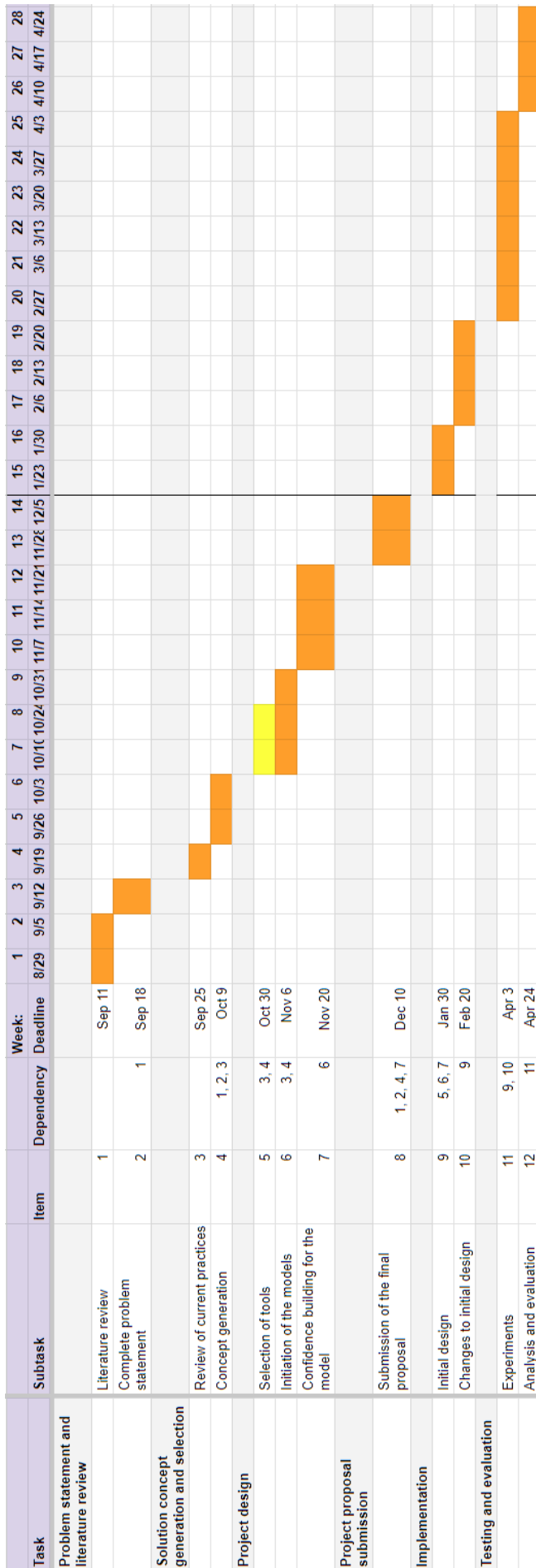


Figure 9.9: Gantt chart and critical path (in orange)